A species of planar triangular tilings with inflation factor $\sqrt{-\tau}$

Ludwig Danzer
and
Gerrit van Ophuysen

May 1999

Dedicated to Branko Grünbaum
on the occasion of his seventieth birthday

Summary: A rather simple species of planar tilings by rectangular triangles – all similar to each other and of only two sizes – is described from three different points of view: As defined by an inflation, as defined using a local matching rule and as defined by the cut and project method. — In accordance with the fact that $\sqrt{-\tau}$ is a complex PV-number, the Fourier-transform of the autocorrelation function turns out to be “strictly point” (i.e. consisting of DIRAC-deltas only). Hence the species is q u a s i periodic.

Contents

1 Introduction

A tiling is said to be *aperiodic*, if it does not admit any translation $(\neq 0)$. It is called *quasiperiodic*, if it is aperiodic and the Fouriertransform of its autocorrelation function consists of Dirac deltas only, provided their support is dense everywhere. We asked ourselves: What is the simplest set of prototiles with an inflation that produces planar tilings which are necessarily not only aperiodic but even q u a s i periodic? For this purpose the inflation factor η has to be a PV-number and must not be a natural number [1)] (see [10]). Therefore it cannot be the square-root of a rational number. Thus the inflation matrix cannot be 1×1 and we need at least two prototiles. To make the example as simple as possible, we take exactly two tiles A and X and require X to be the inflation of A. So we have a small and a large prototile. The inflation matrix with minimal entries then is

$$M := \begin{pmatrix} 0 & 1 \\ 1 & 1 \end{pmatrix}. \tag{1}$$

Here the first column states $\text{infl}(A) := X$ while the second column expresses, that $\text{infl}(X)$ consists of one copy of A and one copy of X. Our realization is shown in Figure 1. The only other one (except similar copies) we know of, is the pair of “chairs” due to R. AMMANN (see [2] chapter 10.4, also cf. Section 6.4).

$A :=$ 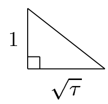

$\text{infl}(A) := X :=$ 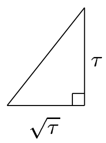

$= \beta(A); \qquad \beta(x) := \begin{pmatrix} 0 & -\sqrt{\tau} \\ \sqrt{\tau} & 0 \end{pmatrix} x; \quad \det(\beta) = \tau := \frac{1+\sqrt{5}}{2}$

$\text{infl}(X) :=$ 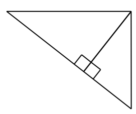
$= \psi_1(X) \,\dot{\cup}\, \psi_2(A)$

$$\psi_1(x) := \begin{pmatrix} -\tau^{-1} & -\tau^{-\frac{1}{2}} \\ -\tau^{-\frac{1}{2}} & \tau^{-1} \end{pmatrix} x - \begin{pmatrix} \tau^{-\frac{1}{2}} \\ 1 \end{pmatrix}; \quad \psi_2 := -\psi_1; \quad \det(\psi_i) = -1$$

Figure 1: Definition of the Inflation

Probably quite a few geometers have found this example too (see e.g. [8] Anhang B.5); but it seems, nobody has studied it in detail, maybe because the resulting tilings are not vertex-to-vertex.

---

[1]) in which case the tilings become either periodic or l i m i t periodic

2 Basic definitions and first consequences

Our *protoset* is $\mathfrak{F} := \{A, X\}$. By *inflation* we denote the substitution as described by Figure 1. Here β is an expansive map with $|\beta(x)| = \sqrt{\tau}|x|$ for all x and the $\psi_i(x) = \varphi_i(x) + t$ are isometries. The translation t has to be replaced by some t_1, t_2 if the origin is not chosen to be the rightangled vertex of A. The only property of the translations worth mentioning is, that they are in a special $\mathbb{Z}$-module (cf. Section 6). In contrast the two reflections φ_1 and φ_2 (cf. Fig. 2), more precisely the directions of their lines of reflection, play an essential rôle in the background of all our considerations. These directions are given by the bisectors of the angles whose tangens equals $\sqrt{\tau}$ of the two tiles and especially will be used in Section 7.3.

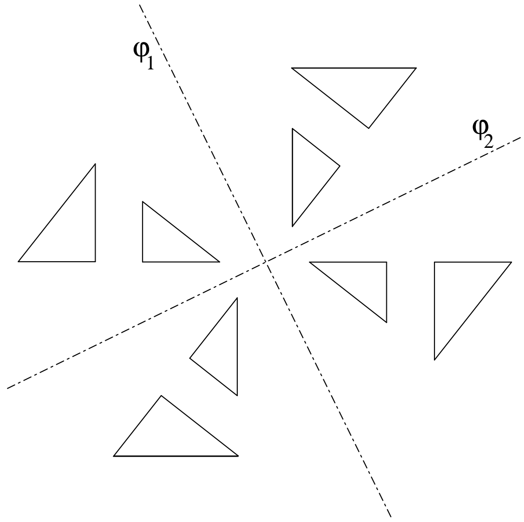

Figure 2: The reflections φ_i acting on a translate of A and a translate of X

$$\mathrm{infl}^3(A) = \mathrm{infl}^2(X) =$$

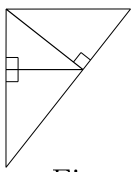

$$= \beta\psi_1\beta^{-1}\psi_1(X) \,\dot{\cup}\, \beta\psi_1\beta^{-1}\psi_2(A) \,\dot{\cup}\, \beta\psi_2\beta^{-1}(X)$$

Figure 3: Iterated Inflation

The inflation infl can be iterated, i.e. the expansion map β, the isometries ψ_1 and ψ_2 and the split of $\beta(X)$ into $\psi_1(X) \,\dot{\cup}\, \psi_2(A)$ have to be applied again as shown in Figure 3.

Definition 1: *The* species $\boldsymbol{\mathcal{S}}(\mathfrak{F}, \mathrm{infl})$ *is the set of all global tilings* $\mathcal{P}$*, where every tile is congruent either to* A *or to* X *and every bounded cluster of* $\mathcal{P}$ *has a congruent counterpart in some* $\mathrm{infl}^n(A)$ *(cf. Fig. 17 and Fig. 10* [2]*). The clusters congruent to* $\mathrm{infl}^n(A)$ *and* $\mathrm{infl}^n(X)$ *are called* supertiles of nth order *(of* A *or* X *resp.).*

[2]) The letters $B, C, \ldots, Z$ and the highlighted figures will be explained in section 5.2.

Obviously the inflation factor η (by which the tiles are expanded in every step) is just $\sqrt{\tau}$.

When the plane is considered as $\mathbb{C}^1$ instead of $\mathbb{E}^2$, the rotation by $90°$ must be taken into account and η becomes $\boldsymbol{i}\sqrt{\tau}$. Since the only algebraic conjugates are $\bar{\eta}$ $(=-\eta)$, $\tau^{-\frac{1}{2}}$ and $-\tau^{-\frac{1}{2}}$ (both in absolute value smaller than one), this is a *complex PV-number.* Therefore (see [10]) the Fourier-transform of the autocorrelation function of the set of all vertices has to have sharp spots. They correspond to the Bragg-Peaks of the diffraction pattern of a material, whose atoms sit at the vertices. For more details cf. Section 6.5. Until then we stay in $\mathbb{E}^2$ with $\eta = \sqrt{\tau}$.

By *deflation* (defl) we denote an inverse process to a given inflation. It can be applied only under the assumption, that the given tiling (or cluster resp.) can be considered as a tiling of *supertiles.* Then each supertile is considered as o n e tile and the whole tiling (cluster) is shrunk by the factor η. An essential question is always, whether the original tiling can be split into supertiles at all, and if so, whether the splitting is unique or not. It is well known, that the deflated tiling – i f the deflation was unique – again belongs to the original inflation species and in fact, then

$$\mathrm{defl} \circ \mathrm{infl} = \mathrm{infl} \circ \mathrm{defl} = \mathrm{id}\,. \tag{2}$$

Remark 1: *The species $\boldsymbol{\mathcal{S}}(\mathfrak{F}, \mathrm{infl})$ has a locally defined u n i q u e deflation.*

Indeed: Due to the 0 in the inflation matrix M (cf. (1)) every small tile is face-to-face with a large tile making up a supertile of X. The remaining large tiles must be considered as supertiles of A.

It is well known that Remark 1 implies

Remark 2: *The species $\boldsymbol{\mathcal{S}}(\mathfrak{F}, \mathrm{infl})$ is aperiodic.*

Remark 3a: *In $\boldsymbol{\mathcal{S}}(\mathfrak{F}, \mathrm{infl})$ there are precisely six congruence classes of vertex stars (vts), as shown in Figure 4.*

Proof: By definition every vertex star of our species has to occur in some $\mathrm{infl}^n(A)$. The first interior vertex occurs in $\mathrm{infl}^5(A)$, the sixth in $\mathrm{infl}^{10}(A)$, but $\mathrm{infl}^{11}(A)$ does not contain a new vertex star, and therefore $\mathrm{infl}^{10+n}(A)$ cannot contain any new vertex star for $n \in \mathbb{N}$. □

From Figure 4 we can also read off

Remark 3b: *For every $n \leq 6$ the rectangular cluster $\mathcal{R}^n := \mathrm{infl}^n(X \dot\cup X) = \mathrm{infl}^n(X) \dot\cup \mathrm{infl}^n(X)$ [3)] is centrally symmetric and contains on its diagonal two vertex stars congruent to $\mathcal{V}^n$.*

[3]) For brevity here and in the sequel we suppress the isometries which actually had to be applied.

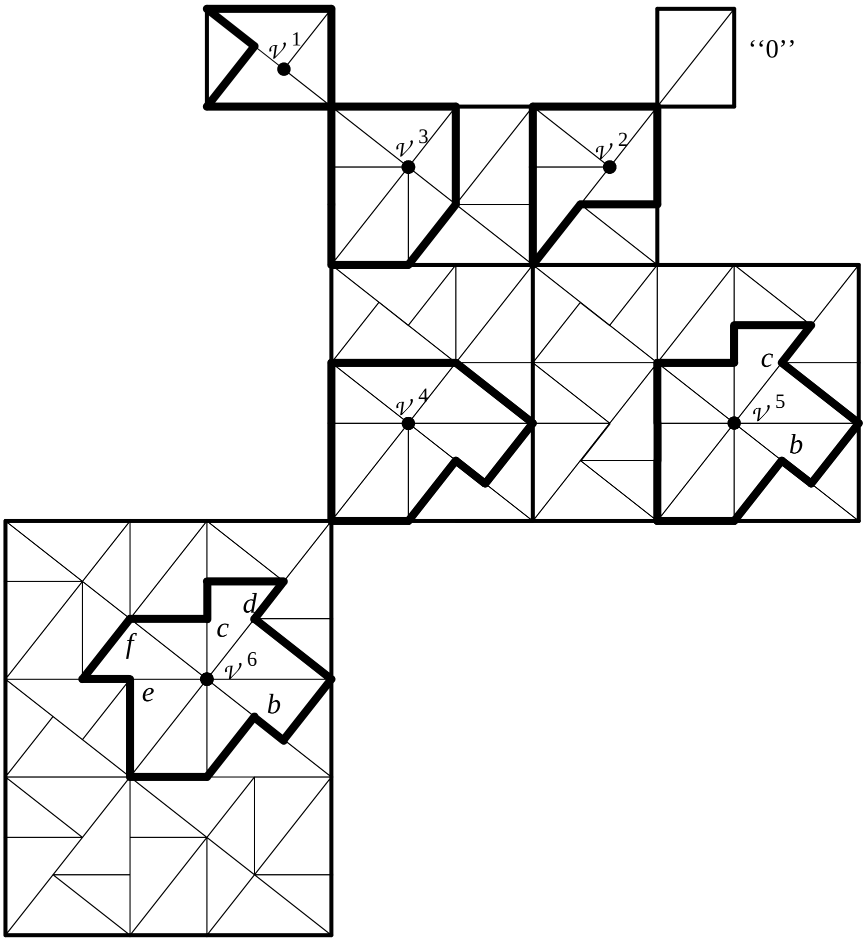

Figure 4: The vertex stars $\mathcal{V}^1$, $\mathcal{V}^2$, $\ldots \mathcal{V}^6$ ($\mathcal{V}^7$ is congruent to $\mathcal{V}^6$) and the rectangles $\mathcal{R}^1, \mathcal{R}^2, \ldots, \mathcal{R}^6$. (This is essentially an excerpt of Fig. 10 not yet colored)

$$\left.\begin{array}{l}\text{Since } X \text{ is as well a supertile } (\mathrm{infl}(A)) \text{ as a tile itself, we use from now} \\ \text{on the term } \textit{supertile of } n\textit{-th order} \text{ only as abbreviation for “} \mathrm{infl}^n(X) \text{”.}\end{array}\right\} \quad (3)$$

3 Properties of $\mathcal{V}^1, \ldots, \mathcal{V}^6$ and clusters enforced by them

We begin with a general definition of what we call a *local matching rule (lmr)*.

Definition 2: *Given a finite protoset* $\mathfrak{F}$ *and a finite set* [4] lmr *of* $\mathfrak{F}$*-clusters, each fitting into a ball of radius* ρ*, we define the species*

$$\boldsymbol{\mathcal{S}}(\mathfrak{F}, \mathrm{lmr})$$

as the set of all global tilings $\mathcal{P}$ *, where every cluster of* $\mathcal{P}$ *which fits into a ball of radius* ρ *has a congruent counterpart in* lmr.

[4]) In this context we speak of an *atlas*.

The reader may note the similarity to Definition 1 and also the differences: In Definition 1 the clusters were not uniformly bounded and the atlas was not finite.

Definition 3: *A cluster $\mathcal{C}$ is said to enforce the cluster $\mathcal{D}$ (with respect to* lmr *), if in every tiling of $\boldsymbol{\mathcal{S}}(\mathfrak{F}, \mathrm{lmr})$ every congruent copy of $\mathcal{C}$ is contained in a $\mathcal{D}$, and everywhere in the same way.* [5)]

In the sequel let lmr_{vi} denote the atlas consisting of the six vertex stars (vts) $\mathcal{V}^1, \ldots, \mathcal{V}^6$ of $\boldsymbol{\mathcal{S}}(\mathfrak{F}, \mathrm{infl})$.

From Figure 4 we can read off directly

Remark 4: *The six vts defined by our inflation can be distinguished by the following facts.*

(a) $\mathcal{V}^1$ *is the only vts whose vertex splits the middle edge of a large tile.*

(b) $\mathcal{V}^2$ *is the only vts, whose vertex splits the hypotenuse of a large tile.*

(c) $\mathcal{V}^1, \mathcal{V}^2$ *are the only vts with a flat angle. They do not contain any rectangle.*

(d) $\mathcal{V}^3$ *is the only vts containing a parallelogram formed by two small tiles sharing their shortest edge.*

(e) $\mathcal{V}^1, \mathcal{V}^3$ *are the only vts with two right angles.*

(f) $\mathcal{V}^5, \mathcal{V}^6$ *are the only vts without any right angle (i.e.: with eight tiles) and the only vts containing the cluster shown in Figure 5(a). Caution:* $\mathcal{V}^6$ *contains* t w o *of them.*

(g) $\mathcal{V}^4$ *is the only vts containing a parallelogram formed by two large tiles sharing their shortest edge. Consequently the cluster shown in Figure 5(b) does not occur at all.*

(h) $\mathcal{V}^5$ *is the only vts containing a rectangle formed by two small tiles.*

(i) *The cluster shown in Figure 5(c) occurs in* $\mathcal{V}^6$ *only and there only once.*

(j) *The configuration shown in Figure 5(d) does not occur in any vts.*

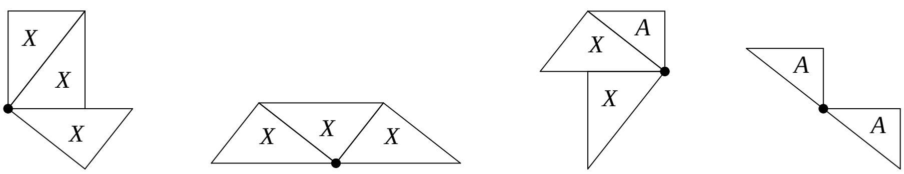

(a) (b) (c) (d)

Figure 5: Some characteristic configurations

Remark 5: *In $\boldsymbol{\mathcal{S}}(\mathfrak{F}, \mathrm{lmr}_{vi})$ we can state:*

$$\mathcal{V}^i \quad \textit{enforces} \quad \mathcal{R}^i \qquad (1 \le i \le 5) \tag{4.i}$$

$$\mathcal{V}^6 \quad \textit{enforces} \quad \mathcal{C}^6 \qquad \textit{(cf. Fig. 6)}. \tag{5}$$

[5]) The largest such cluster $\mathcal{D}$ usually is called the *empire* of $\mathcal{C}$ (w.r.t. lmr).

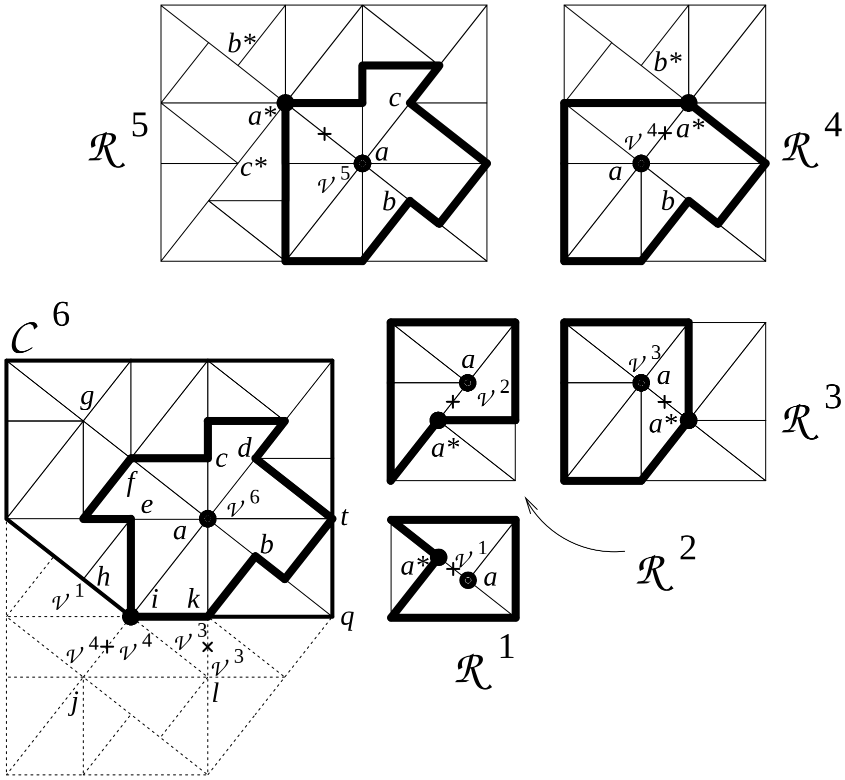

Figure 6: Clusters enforced by the vertex stars

Proof: (4.1) follows from Remark 4(a).

(4.2) follows from Remark 4(b).

(4.3) follows from Remark 4(d).

(4.4) follows from Remark 4(a) – applied at the vertex b – and Remark 4(g).

(4.5) follows from Remark 4(h), Remark 4(a) applied at b, Remark 4(b) applied at c and finally (4.1) and (4.2).

Ad (5): In the same manner as above the vertices b and c lead to two copies of $\mathcal{R}^1$, d and e to two copies of $\mathcal{R}^2$; and finally $\mathcal{C}^6$ is completed due to Remark 4(e) – applied at f – and (4.3). □

Remark 6: *If $\mathcal{C}^6$ is given as shown in Figure 6, then there are precisely the following three possibilities:*

$$\left.\begin{array}{l}\mathcal{V}(i) \cong \mathcal{V}^6 \text{ and } \mathcal{C}^6 \text{ is contained in a copy of } \mathcal{R}^6 \text{ centered at } \tfrac{1}{2}(i+a)\,.\\ \text{In this case } \mathcal{V}(h) \cong \mathcal{V}^1 \text{ and } \mathcal{V}(k) \cong \mathcal{V}^2\,.\end{array}\right\} \quad (6.1)$$

$$\left.\begin{array}{l}\mathcal{V}(i) \cong \mathcal{V}^4 \text{ and } \mathcal{C}^6 \text{ is contained in } \mathrm{infl}(\mathcal{C}^6) \text{ as shown in Figure 6 (in-}\\ \text{cluding the dotted lines). In this case } \mathcal{V}(h) \cong \mathcal{V}^1 \text{ and } \mathcal{V}(k) \cong \mathcal{V}^3\,.\end{array}\right\} \quad (6.2)$$

$$\left.\begin{array}{l}\mathcal{V}(i) \cong \mathcal{V}^3\,. \text{ In this case the full cluster of Figure 7 is enforced, and}\\ \text{again } \mathcal{V}(k) \cong \mathcal{V}^3\,.\end{array}\right\} \quad (6.3)$$

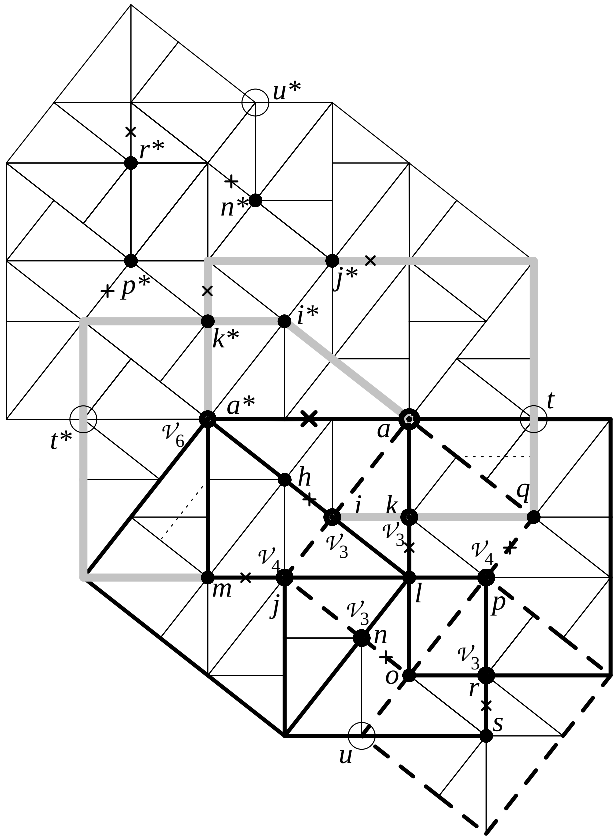

Figure 7: The case where at i there is a $\mathcal{V}^3$

Proof: Obviously $\mathcal{V}(i) \not\cong \mathcal{V}^1, \mathcal{V}^2$. If $\mathcal{V}(i)$ were of type $\mathcal{V}^5$, we should have - due to Remark 5 (4,5) – an $\mathcal{R}^5$ with $\mathcal{V}(k) \cong \mathcal{V}^1$. ↯

Ad (6.1): By Remark 5 (5) we have two overlapping clusters of type $\mathcal{C}^6$. Their union is $\mathcal{R}^6$.

Ad (6.2): By Remark 5 (4,4) $\mathcal{V}(i)$ enforces the $\mathcal{R}^4$ centered at $\frac{1}{2}(j+i)$. It follows $\mathcal{V}(k) \cong \mathcal{V}^3$ (cf. Remark 4(e)) and consequently we have the $\mathcal{R}^3$ centered at $\frac{1}{2}(l+k)$.

Ad (6.3): In this case $\mathcal{V}(i)$ enforces the $\mathcal{R}^3$ centered at $\frac{1}{2}(h+i)$. Since in the triangle $\triangle ail$ this cluster coincides with the $\mathcal{R}^4$, we still have the $\mathcal{R}^3$ centered at $\frac{1}{2}(l+k)$.

Next consider the vertex denoted by a^* in Figure 7. Due to Remark 4(i) $\mathcal{V}(a^*) \cong \mathcal{V}^6$ and consequently we have another $\mathcal{C}^6$. Because $\mathcal{V}(i^*)$ was $\cong \mathcal{V}^3$ already before, we have now symmetry with respect to $\frac{1}{2}(a^*+a)$, and everything we shall prove in the “South”, will automatically apply for the “North” as well.

At j both, a $\mathcal{V}^3$ or a $\mathcal{V}^4$ seem possible. But a $\mathcal{V}^3$ would require a $\mathcal{V}^4$ at m including the dotted A there. Hence $\mathcal{V}(j) \cong \mathcal{V}^4$ and we have got the $\mathcal{R}^4$ centered at $\frac{1}{2}(m+j)$.

Now at n we have the same situation as before at k , whence $\mathcal{V}(n) \cong \mathcal{V}^3$ and we get an $\mathcal{R}^3$ centered at $\frac{1}{2}(o+n)$. As before at j a $\mathcal{V}^3$ at p would create a contradiction at q (cf. the dotted A there). Therefore $\mathcal{V}(p) \cong \mathcal{V}^4$ and we have the $\mathcal{R}^4$ centered at $\frac{1}{2}(q+p)$. Finally we can conclude $\mathcal{V}(r) \cong \mathcal{V}(s) \cong \mathcal{V}^3$. □

The cluster of Figure 7 is not the complete empire of $\mathcal{V}(a) \cup \mathcal{V}(i)$; but at least locally at t , u , t^* and u^* as well $\mathcal{V}^3$ s as $\mathcal{V}^4$ s are possible.

4 The species $\boldsymbol{\mathcal{S}}(\mathfrak{F}, \mathrm{infl})$ cannot be defined by a local matching rule

The following theorem and its proof are typical for many inflation species. Its statement, that our original species cannot be described by any lmr, will be the motivation to introduce *colours* in the next section.

Theorem 1: $\boldsymbol{\mathcal{S}}(\mathfrak{F}, \mathrm{infl})$ *cannot be defined by any local matching rule (* lmr *). More precisely: There is no* lmr *with* $\boldsymbol{\mathcal{S}}(\mathfrak{F}, \mathrm{lmr}) = \boldsymbol{\mathcal{S}}(\mathfrak{F}, \mathrm{infl})$ *(cf. Def. 2).*

Proof: Assume on the contrary the existence of a radius ρ and an atlas $\boldsymbol{\mathcal{A}}$ of ρ-clusters of A s and X s defining the species $\boldsymbol{\mathcal{S}}(\mathfrak{F}, \mathrm{lmr}_{\boldsymbol{\mathcal{A}}})$, and assume

$$\boldsymbol{\mathcal{S}}(\mathfrak{F}, \mathrm{lmr}_{\boldsymbol{\mathcal{A}}}) = \boldsymbol{\mathcal{S}}(\mathfrak{F}, \mathrm{infl}). \tag{7}$$

This implies that both species contain precisely the same six congruence classes of vts.

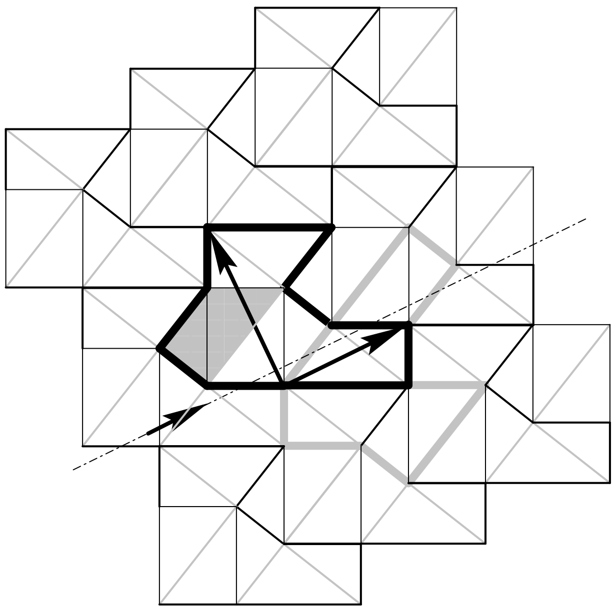

Figure 8: A periodic tiling of the plane using vertex star $\mathcal{V}^3$ only

Now consider the crystallographic [6)] tiling $\mathcal{P}$ shown in Figure 8. All vts of $\mathcal{P}$ are congruent to $\mathcal{V}^3$. Furthermore $\mathcal{P}$ is invariant under the glidereflection symbolized by the short arrow lying on the axis of the reflection. Its direction is that of the reflection line of φ_2 mentioned in Section 2.

[6)] i. e. d o u b l y periodic.

It is easily checked that in every tiling which has no other than our six vts,

$$\left.\begin{array}{l}\text{for every ball with radius at most } \frac{1}{2}\tau^{-1} \text{ there is at least one vertex star,}\\ \text{which covers the ball completely }^{7)}.\end{array}\right\} \qquad (8)$$

In particular every ball of radius $.3$ is covered by some vertex star of $\mathcal{P}$.

Finally consider the tiling $\mathcal{Q} := \text{infl}^n(\mathcal{P})$, where $\eta^n \cdot .3 = \tau^{\frac{n}{2}} \cdot .3 > \rho$. Thus in $\mathcal{Q}$ every ball of radius ρ is covered by a copy of $\text{infl}^n(\mathcal{V}^3)$, and from (7) and the definition of $\text{lmr}_{\mathcal{A}}$ we conclude $\mathcal{Q} \in \boldsymbol{\mathcal{S}}(\mathfrak{F}, \text{lmr}_{\mathcal{A}})$. But since $\mathcal{Q}$ is periodic, while our inflation species is aperiodic (cf. Remark 2) this contradicts (7). □

5 Colouring does help

5.1 A coloured inflation species

After the papers [7] by Ch. Radin and [12] by Ch. Goodman-Strauss the next to do is, to find a *colouring* of $\boldsymbol{\mathcal{S}}(\mathfrak{F}, \text{infl})$ that does permit a local matching rule. In principle it would be "enough" to colour every member of our species and then find a radius ρ such that the atlas $\boldsymbol{\mathcal{A}}$ of all coloured ρ-clusters (used as an lmr) does not permit any new tiling, without caring about an inflation of the coloured tilings. This would correspond to the very general result by Goodman-Strauss, which doubtless was a break-through. In our particular case we are going to prove a somewhat stronger result [8]. We want to replace A and X by finitely many congruent copies with different colours, k e e p the old inflation g e o m e t r i c a l l y and then colour the supertiles of first order in such a way, that the – now coloured – vertex stars (vts) can serve as an atlas lmr_{vic} for the coloured inflation species. So it will become an inflation species with local matching rules, which – after erasing the colours – will coincide with our original species. This can be done as follows.

We define a *coloured* protoset

$$\mathfrak{F}_c := \{A, B, C, D, E; V, W, X, Y, Z\}, \qquad (9)$$

where A is our old A while B, C, D, E are congruent to A, and likewise X is our old X and the others are congruent to X. Next we define a *coloured* inflation by

$$\left.\begin{array}{rclrcl}\text{infl}_c(A) & := & V; & \text{infl}_c(V) & := & B \,\dot\cup\, W;\\ \text{infl}_c(B) & := & W; & \text{infl}_c(W) & := & A \,\dot\cup\, Y;\\ \text{infl}_c(C) & := & X; & \text{infl}_c(X) & := & E \,\dot\cup\, V;\\ \text{infl}_c(D) & := & Y; & \text{infl}_c(Y) & := & D \,\dot\cup\, X;\\ \text{infl}_c(E) & := & Z; & \text{infl}_c(Z) & := & C \,\dot\cup\, Z\ ^{9)}.\end{array}\right\} \qquad (10)$$

[7]) It can be shown, that for inflation species satisfying some rather general conditions there is always such a radius.

[8]) It may well be, that a closer inspection of [12] will show, that his techniques give this "inflation extending colouring" in general.

This implies (in the sequel we omit the symbol "$\dot\cup$")

$$\left.\begin{array}{rclrcl} \mathrm{infl}_c^2(V) & := & WAY; & \mathrm{infl}_c^3(V) & := & AYVDX; \\ \mathrm{infl}_c^2(W) & := & VDX; & \mathrm{infl}_c^3(W) & := & BWYEV; \\ \mathrm{infl}_c^2(X) & := & ZBW; & \mathrm{infl}_c^3(X) & := & CZWAY; \\ \mathrm{infl}_c^2(Y) & := & YEV; & \mathrm{infl}_c^3(Y) & := & DXZBW; \\ \mathrm{infl}_c^2(Z) & := & XCZ; & \mathrm{infl}_c^3(Z) & := & EVXCZ; \end{array}\right\} \qquad (11)$$

and

$$\left.\begin{array}{l} \mathrm{infl}_c^4(V) := VDXBWYEV; \\ \mathrm{infl}_c^5(V) := BWYEVWAYDXZBW; \\ \mathrm{infl}_c^6(V) := WAYDXZBWAYVDXYEVCZWAY. \end{array}\right\} \qquad (12)$$

Obvously the small prototiles $A,\ldots,E$ as well as the large prototiles $V,\ldots,Z$ are cyclically permuted by

$$\pi := (ABCDE)(VYWZX). \qquad (13)$$

This permutation has the following remarkable property: For e v e r y prototile T

$$\pi(\mathrm{infl}_c(T)) = \mathrm{infl}_c(\pi^3(T)). \qquad (14)$$

By induction we conclude

$$\pi^k(\mathrm{infl}_c(T)) = \mathrm{infl}_c(\pi^{3k}(T)) \qquad \text{(for } k \in \mathbb{N}\text{)} \qquad \text{and} \qquad (15)$$

$$\pi(\mathrm{infl}_c^n(T)) = \mathrm{infl}_c(\pi^{3^n}(T)) \qquad \text{(for } n \in \mathbb{N}\text{)}. \qquad (16)$$

Since $3^n \not\equiv 0 \pmod 5$ for all n this implies:

The species $\boldsymbol{\mathcal{S}}(\mathfrak{F}_c, \mathrm{infl}_c)$ is invariant under the group $\mathcal{A}ut_c$ generated by π. (17)

Hence we need not give (12) for $W,\ldots,Z$ instead of V. To understand what neighbourhoods occur in our coloured inflation species we show in Figure 9 $\mathrm{infl}_c^n(Y)$ for $1 \le n \le 10$ and highlight successively the new neighbourhoods. Only these can be germs for new neighbourhoods in the next inflation. Therefore for $n \ge 5$ only the higher inflations of the rectangle $\mathcal{R}_c^0(Z,X)$ are given.

From Figure 9 we conclude (cf. the Appendix):

In the entire coloured inflation species every rectangle congruent to $\mathcal{R}^n$ belongs to the type [10] $\mathcal{R}_c^n(Z,X)$ (modulo $\mathcal{A}ut_c$). (18)

---

[9]) An explanation for this strange looking rule will be given in the Appendix. Instead of using ten characters, we could of course use f i v e colours; the same for X as for A.

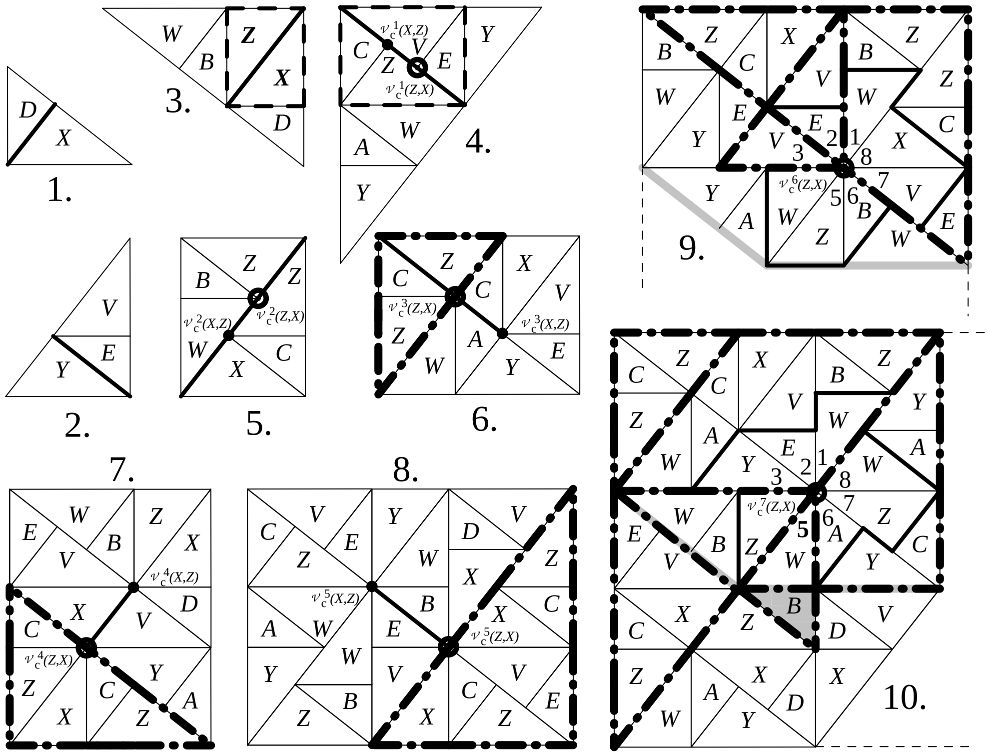

Figure 9: $\text{infl}_c^n(Y)$ for $1 \leq n \leq 10$, the new neighbourhoods (——) and the pseudo-supertiles (–·–) contained therein.

We also observe — and the following statements are of course subject to $\mathcal{A}ut_c$ — :

in $\text{infl}_c^4(Y)$ there is a tile Y at either end homothetic to the carrier of $\text{infl}_c^4(Y)$, (19.1)

and

the two vts $\mathcal{V}_c^n(X, Z)$ and $\mathcal{V}_c^n(Z, X)$ are not of the same type (though of course congruent). (19.2)

In particular for $n \geq 3$ $\mathcal{R}_c^n(X, Z)$ contains $\text{infl}_c^{n-1}(Y)$ in the corner near $\mathcal{V}_c^n(X, Z)$, which is not "naturally" a c-supertile, but only due to the special character of the inflation rule (10). In contrast, in the other corner it contains a cluster congruent to the supertiles of order $n-1$, but n o t of the type of any coloured supertile (cf. Fig. 9.6 - 9.10). Clusters of such a type we shall call *pseudo-* supertiles in the sequel. (19.3)

[10]) In this section we use the term *type* as an abbrevation for "congruence class of ..., all coloured in the same way". We call two clusters *equal*, if they are of the same type. Obviously there are c o n g r u e n t clusters, which are n o t equal.

Every rectangle $\mathcal{R}^n(.,.)$ is the union of two c-supertiles of order n. For $n \geq 3$ it contains three c-supertiles and one pseudo-supertile of order $n-1$ (cf. (3)). (19.4)

These pseudo-supertiles will play an essential rôle in the proof of Theorem 2.

Next we consider the vts of the coloured inflation species defined by (10). Quite a few are contained in Figure 10. We see (and can deduce also from Fig. 9.10), that

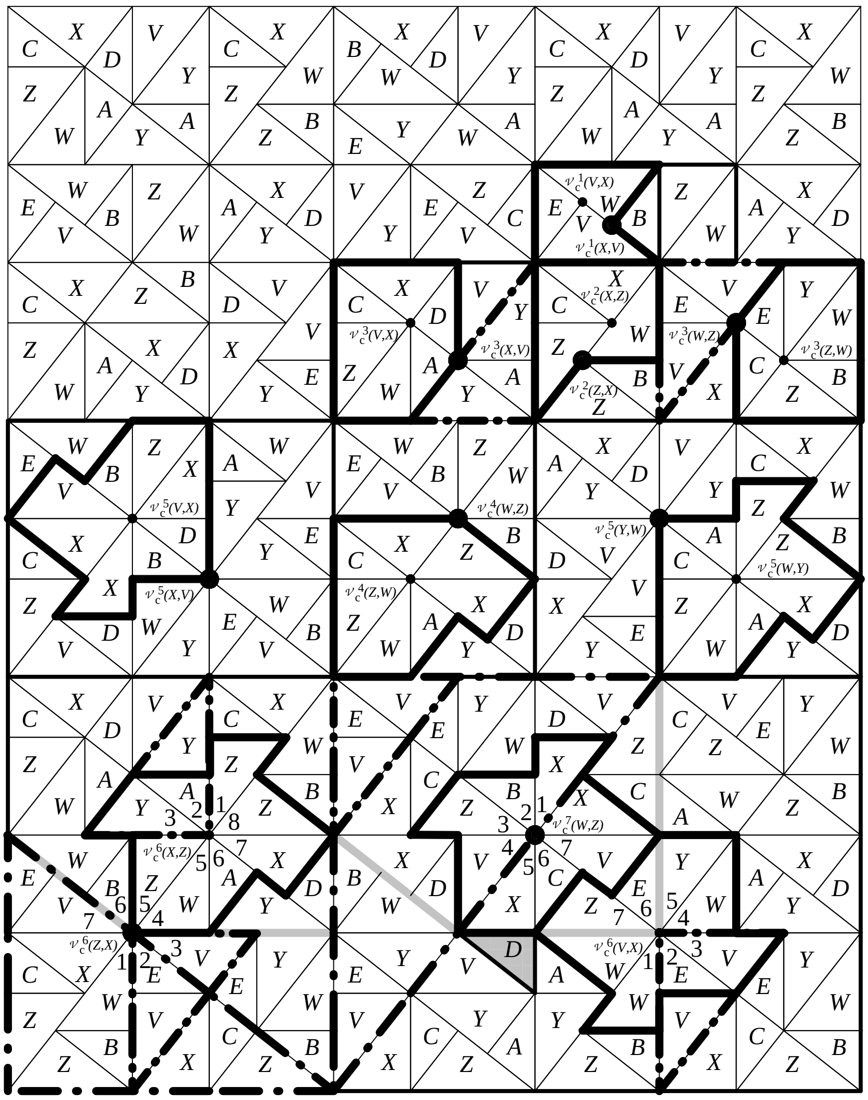

Figure 10: $\mathrm{infl}_c^{10}(Z \dot\cup X)$ ($\mathrm{infl}^{10}(Z)$ upper left, $\mathrm{infl}^{10}(X)$ lower right part)

$\mathcal{V}_c^7(W,Z) \subset \mathrm{infl}_c(\mathcal{V}_c^6(W,Z)$ is a new type, while $\mathcal{V}_c^7(Z,W) = \mathcal{V}_c^6(V,X)$. It is easily checked, that $\mathcal{V}_c^8(W,Z) = \mathcal{V}_c^6(Z,X)$. So we have with respect to infl_c the following "family trees":

$$\begin{array}{ll} \text{Type 1:} & 1 \to 2 \to 3 \to 4 \to 5 \to 6 \rightleftarrows 7 \\ \text{Type 2:} & 1 \to 2 \to 3 \to 4 \to 5 \to 6 \circlearrowleft. \end{array} \qquad (20)$$

Here type 1 is represented modulo $\mathcal{A}ut_c$ by $\mathcal{V}_c(Z,X)$ whose vertex is always on the boundary of a pseudo-supertile, while type 2 is represented by $\mathcal{V}_c(X,Z)$. The vertices with vts of type 1 are highlighted by bold dots in Figures 9 and 10.

We need a complete list of all vts $\trianglelefteq \mathcal{V}^6$. Since (12) is subject to $\mathcal{A}ut_c$ there are 15 of them. For abbreviation we denote e.g. $\mathcal{V}_c^6(X,Z)$ by

$$ZAYZ|WAXZ \qquad \text{(cf. Fig. 10).} \tag{21}$$

The first place in this code corresponds to the large tile, whose middle edge is split by a $\mathcal{V}_c^1$, the second place to the small tile, which belongs to this $\mathcal{V}_c^1$, etc.. We give the complete list:

$$\left.\begin{array}{lclclcl}
\mathcal{V}_c^6(Z,X) &=& W\,E\,V\,W|Z\,B\,V\,X & \quad & \mathcal{V}_c^6(X,Z) &=& Z\,A\,Y\,Z|W\,A\,X\,Z \\
\mathcal{V}_c^6(X,V) &=& Y\,D\,X\,Y|W\,A\,X\,Z & & \mathcal{V}_c^6(V,X) &=& W\,E\,V\,W|Y\,E\,Z\,W \\
\mathcal{V}_c^6(V,Y) &=& V\,C\,Z\,V|Y\,E\,Z\,W & & \mathcal{V}_c^6(Y,V) &=& Y\,D\,X\,Y|V\,D\,W\,Y \\
\mathcal{V}_c^6(Y,W) &=& X\,B\,W\,X|V\,D\,W\,Y & & \mathcal{V}_c^6(W,Y) &=& V\,C\,Z\,V|X\,C\,Y\,V \\
\mathcal{V}_c^6(W,Z) &=& Z\,A\,Y\,Z|X\,C\,Y\,V & & \mathcal{V}_c^6(Z,W) &=& X\,B\,W\,X|Z\,B\,V\,X \\
 & & & & & & \\
\mathcal{V}_c^7(Z,X) &=& W\,E\,Y\,Z|W\,A\,Z\,W & & & & \\
\mathcal{V}_c^7(X,V) &=& V\,C\,X\,Y|V\,D\,Y\,V & & & & \\
\mathcal{V}_c^7(V,Y) &=& Z\,A\,W\,X|Z\,B\,X\,Z & & & & \\
\mathcal{V}_c^7(Y,W) &=& Y\,D\,V\,W|Y\,E\,W\,Y & & & & \\
\mathcal{V}_c^7(W,Z) &=& X\,B\,Z\,V|X\,C\,V\,X & & & &
\end{array}\right\} \tag{L}$$

We close this section by

Remark 7: *If in a c-supertile of any order the colour of any one tile is given, the colouring of the whole c-supertile is determined.*

This is an immediate consequence of (17): There are only five c-supertiles of every order and at every place every colour occurs just once. □

5.2 The corresponding coloured lmr-species

We define the *coloured* local matching rule lmr_{vic} by the atlas made up by the 65 coloured vertex stars (vts) of the coloured inflation species considered in Subsection 5.1 . We want to prove

Theorem 2: $$\boldsymbol{\mathcal{S}}(\mathfrak{F}_c, \mathrm{lmr}_{vic}) = \boldsymbol{\mathcal{S}}(\mathfrak{F}_c, \mathrm{infl}_c)\,.$$

Obviously this implies the

Corollary : $\boldsymbol{\mathcal{S}}(\mathfrak{F}, \mathrm{infl})$ *can be defined as* $F(\boldsymbol{\mathcal{S}}(\mathfrak{F}_c, \mathrm{lmr}_{vic}))$, *where* F *is the "forget functor" with respect to the colours.*

Before we start with the proof of the theorem itself we premise five remarks and a crucial lemma. In all these statements the silent prerequisite is, that we are in $\boldsymbol{\mathcal{S}}(\mathfrak{F}_c, \mathbf{lmr}_{\boldsymbol{vic}})$ and not yet in the desired inflation species and that our structures occur in a global tiling.

Remark $\mathbf{5_c}$: *For $1 \leq n \leq 5$ $\mathcal{V}_c^n(.,.)$ enforces the corresponding c o l o u r e d rectangle $\mathcal{R}_c^n(.,.)$. In the same sense for $6 \leq n \leq 7$ $\mathcal{V}_c^n(.,.)$ enforces $\mathcal{C}_c^n(.,.)$ (cf. Def. 3).*

The proof is quite analogous to the proof of Remark 5. At every step the colour of two tiles, one tile at e i t h e r side of the principal diagonal, is known already. Hence only one of the ten congruent coloured vts will fit. □

Remark 8: *Let $\mathcal{D}$ be a cluster congruent to a supertile of first order (cf.* (3)*) in a tiling of $\boldsymbol{\mathcal{S}}(\mathfrak{F}_c, \mathrm{lmr}_{vic})$; then $\mathcal{D}$ is a c-supertile. In other words: There are no pseudo-supertiles of first order.*

Proof: Consider the vertex x, where the two right angles are. Due to Remark 4(e) $\mathcal{V}(x) \cong \mathcal{V}^1$ or $\mathcal{V}^3$. In both cases $\mathcal{D}$ lies completely on one side of the principal diagonal of the corresponding rectangle, and therefore is a c-supertile. □

Remark 9: (a) *Let $\mathcal{D}$ be a cluster congruent to a supertile of order two and let x be its rightangled vertex. Further assume $\mathcal{V}_c(x)$ to be of order n different from 6 ($n \leq 7$). Then $\mathcal{D}$ is a c-supertile.*

(b) *The same holds, in case $\mathcal{V}_c(x) = \mathcal{V}_c^6(.,.)$, if $\mathcal{D}$ contains the tiles in place 5 and place 6 in our list* (L).

(c) *The cluster $\mathcal{D}$ is a p s e u d o -supertile, if and only if $\mathcal{V}_c(x) = \mathcal{V}_c^6(.,.)$ and $\mathcal{D}$ contains the tiles numbered 2 and 3 in* (L).

Proof: In all cases of part (a) and (b) $\mathcal{D}$ is a natural subsupertile of one of the two c-supertiles of order n, which constitute the rectangle in which $\mathcal{V}_c(x)$ is contained. The only case not covered by (a) and (b) is (c) (cf. Fig. 10). The "if-part" of (c) is true, since it is true for $\mathcal{V}_c^6(X,Z)$ and for $\mathcal{V}_c^6(Z,X)$. □

Remark 10: *Whenever a vts $\mathcal{V}_c^7(.,.)$ occurs in $\boldsymbol{\mathcal{S}}(\mathfrak{F}_c, \mathrm{lmr}_{vic})$ the tile in place 5 of our code is part of a c-supertile of first order (cf. the small shadowed tiles in Figs 9.10 and 10).*

Proof: W.l.o.g. we consider only $\mathcal{V}_c^7(Z,X)$, the one of Figure 9.10. Due to Remark $\mathbf{5_c}$ it enforces $\mathcal{C}_c^7(Z,X)$ (cf. Fig. 11). If Remark 10 were false, due to Remark 8 we should have

$$\mathcal{V}(k) \not\cong \mathcal{V}^3. \tag{22}$$

Applying Remark 6 we conclude $\mathcal{V}(k) \cong \mathcal{V}^2$ and $\mathcal{V}(i) \cong \mathcal{V}^6$. Since the code of $\mathcal{V}(i)$ has to be $\ldots W|ZB\ldots$, we get $\mathcal{V}_c(i) = \mathcal{V}_c^6(Z,X)$. It follows $\mathcal{V}(q) \cong \mathcal{V}^5$ or $\mathcal{V}^6$ (cf. Remark 4(f)). If $\mathcal{V}(q)$ were a $\mathcal{V}^5$, the triangle $\triangle iqv$ had to be a c-supertile. Since it is not, we conclude $\mathcal{V}(q) \cong \mathcal{V}^6$ with code $YC\ldots|\ldots WY$. But such a code does not exist in the list (L) and hence (22) must be false. □

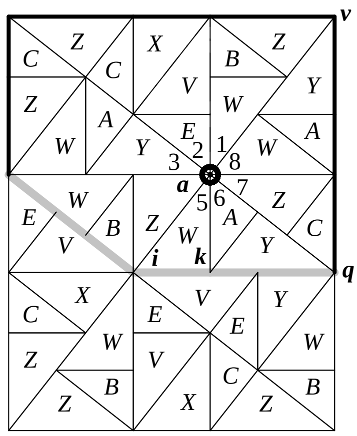

Figure 11: Proof of Remark 10

Lemma : *Let $\mathcal{R}_c^3$ be a rectangle of order three in a tiling of $\boldsymbol{\mathcal{S}}(\mathfrak{F}_c, \mathrm{lmr}_{vic})$. Then the two corners of $\mathcal{R}^3$ which lie on its principal diagonal have vts congruent to $\mathcal{V}^6$. (They may by of type $\mathcal{V}^7(.,.)$.)*

Proof: W.l.o.g. we may assume

$$\mathcal{R}_c^3 = \mathcal{R}_c^3(V, X) \tag{P.0}$$

as shown in Figure 12. The little ciphers in the tiles correspond to the order of the arguments in the following considerations. When only the location of a tile is known, but its colour yet unknown, the cipher is in one of its corners. Otherwise it appears as a lower index of the name of the tile.

Since $\triangle ace$ is a pseudo-supertile

$$\mathcal{V}_c(a) = \mathcal{V}_c^6(\ .\ , Z) \qquad \text{(cf. Remark 9(c) and (L))}, \tag{P.1}$$

and we get Figure 12 up to index 1.

Now, due to Remark 4(f), $\mathcal{V}(d)$ has to be either a $\mathcal{V}^5$ or a $\mathcal{V}^6$. In the latter case — since the code $..WW|Z\ ...$ does not exist —, Z_0 must be in place 7 and W_1 in place 1. In either case

we can add the tiles with index 2 in Figure 12 (but yet cannot determine their colours). (P.2)

This shows $\mathcal{V}(b) \not\cong \mathcal{V}^n$ for $n \leq 3$.

Let us assume $\mathcal{V}(b) \not\cong \mathcal{V}^6$. (23)

Consequently

$$\mathcal{V}(b) \cong \mathcal{V}^4 \text{ or } \mathcal{V}^5 \tag{P.3}$$

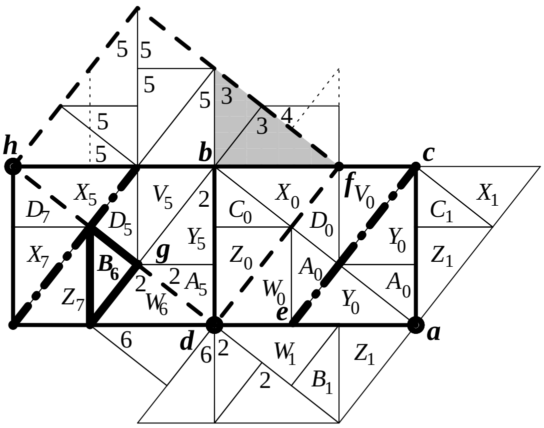

Figure 12: The case $\mathcal{V}(d) \cong \mathcal{V}^6$

and we get the two shadowed tiles at the vertex b. This enforces

$$\mathcal{V}(f) \cong \mathcal{V}^4 \tag{P.4}$$

because, due to Remark 4(c) and 4(f), the only other possibility would be a $\mathcal{V}^3$, leading at c to the configuration of Figure 5(d), which we had excluded.

The new tile at f rules out the case $\mathcal{V}(b) \cong \mathcal{V}^5$, which would require the dotted tile there. So we can state

$$\mathcal{V}(b) \cong \mathcal{V}^4 \text{ and consequently } \mathcal{V}_c(b) = \mathcal{V}_c^4(\,.\,, X). \tag{P.5}$$

Case 1 : $\mathcal{V}(d) \cong \mathcal{V}^6$.

Then, due to (P.5), the code of $\mathcal{V}(d)$ is $W \ldots | \,.\, AZW$ and

$$\mathcal{V}_c(d) = \mathcal{V}_c^7(Z, X) \text{ (cf. (L)), and we may apply Remark 10.} \tag{P.6}$$

This (the highlighted tile B_6) implies

$$\mathcal{V}_c(g) = \mathcal{V}_c^3(Y, V). \tag{P.7}$$

Now — since $X_5 D_7 X_7$ is a pseudo-supertile — we can apply Remark 9(c) once more and see, $\mathcal{V}_c(h)$ has to be a $\mathcal{V}_c^6$ with the tile D_7 in place 2. But this contradicts the configuration at h determined by (P.5). ↯

Case 2 : $\mathcal{V}(d) \cong \mathcal{V}^5$. Then

$$\mathcal{V}_c(d) = \mathcal{V}_c^5(W, Z) \text{ (cf. Fig. 13, which is up to index 5 a copy of Fig. 12).} \tag{P.8}$$

Now the highlighted tile E_8 does not allow $\mathcal{V}(g) \cong \mathcal{V}^3$ (cf. Remark 4(j)). Therefore

$$\mathcal{V}_c(g) = \mathcal{V}_c^4(Y, V). \tag{P.9}$$

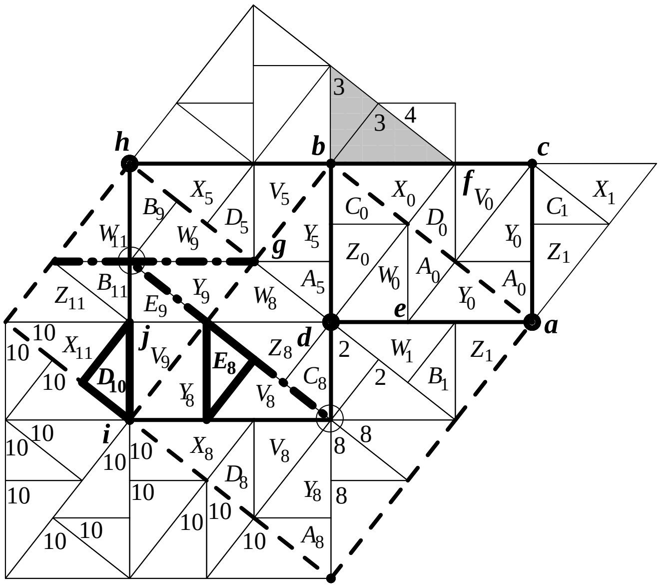

Figure 13: The case $\mathcal{V}(d) \cong \mathcal{V}^5$

Next $\mathcal{V}(i)$ cannot be a $\mathcal{V}^5$, since then the large triangle $\triangle \circ i \circ$ had to be a c-supertile, but is not. Hence $\mathcal{V}(i) \cong \mathcal{V}^6$ with code either $..XY|V...$ or $X...|..VY$. The latter type is not in our list (L) and we conclude

$$\mathcal{V}_c(i) = \mathcal{V}_c^6(Y,V) \textit{ or } \mathcal{V}_c^7(X,V). \tag{P.10}$$

Since these two vts coincide in D_{10}, we get

$$\mathcal{V}_c(j) = \mathcal{V}_c^3(W,Y). \tag{P.11}$$

Now the cluster $W_{11}B_9W_9$ is a pseudo-supertile, and again we end up with

$$\mathcal{V}(h) \cong \mathcal{V}^6 \qquad \text{(cf. Remark 9(c))}. \tag{P.12}$$

The code had to be $....|WBX.$, which does not appear in (L). ↯

This proves (23) to be false. □

Now let $\mathcal{T}$ be an arbitrary lmr_{vic}-tiling. Due to Remark 8 we can define $\mathrm{DEFL}_c(\mathcal{T})$ as follows (cf. the proof of Remark 1) [11]:

Every supertile of first order is considered as o n e tile with the appropriate name given by (10) (BW becomes V etc.). The remaining large tiles are also renamed according to (10) (V becomes A etc.). Finally the whole tiling is shrunk by the factor $\sqrt{\tau}$ and clockwise rotated by $90°$ (i.e. we apply β^{-1}; cf. Fig. 1).

[11]) DEFL_c is n o t defined in terms of infl_c and it must not be considered as left inverse of infl_c; not yet. It is rather an operation deduced from lmr_{vic} (which of course once was derived from infl_c, which is in geometric accordance with infl. The authors regret the somewhat confusing situation.)

Of course the definition is designed to guarantee

$$\mathrm{infl}_c(\mathrm{DEFL}_c(\mathcal{T})) = \mathcal{T}. \tag{24}$$

The crucial rôle of our Lemma becomes evident in the proof of

Remark 11: *If* $\mathcal{T}$ *is a member of* $\boldsymbol{\mathcal{S}}(\mathfrak{F}_c, \mathrm{lmr}_{vic})$, *then so is* $\mathrm{DEFL}_c(\mathcal{T})$.

Proof: It is sufficient to show:

Let a be a vertex of $\mathcal{T}$, $\mathcal{V} := \mathcal{V}_c^n(a)$ its vertex-star ($2 \le n \le 7$) and $\mathcal{W}$ the vts of the corresponding vertex b in $\mathrm{DEFL}_c(\mathcal{T})$; then $\mathcal{W}$ is a member of lmr_{vic} .

Case 1 : All the supertiles of order 1 with vertex a are contained in the corresponding rectangle $\mathcal{R}_c^n(.,.)$ (for $n \le 5$) or in $\mathcal{C}_c^n(.,.)$ (for $n = 6$, 7).

Then $\mathcal{W}$ is contained in $\mathcal{R}_c^{n-1}(.,.)$ (or in $\mathcal{C}_c^6$ or $\mathcal{C}_c^7$ respectively) and therefore it is in lmr_{vic} .

Case 2 : There is a supertile of order 1 with vertex a whose smaller part is outside of $\mathcal{R}_c^n$ ($\mathcal{C}_c^6$, $\mathcal{C}_c^7$ resp.). Then — independent of n — we have the situation of Figure 14. W.l.o.g. we may assume the critical supertile to be of type $\mathrm{infl}_c(Y) = DX$.

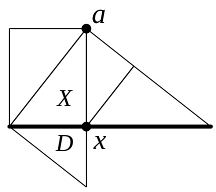

Figure 14: The critical configuration for DEFL_c

From Remark 4(e) we deduce $\mathcal{V}(x) \cong \mathcal{V}^3$, and our Lemma shows

$$\mathcal{V}(a) \cong \mathcal{V}^6. \tag{25}$$

Due to the assumption of case 2 X must be in position 5 in the list (L), and we have either

$$\mathcal{V}_c(a) = \mathcal{V}_c^6(W, Z) \text{ or } \mathcal{V}_c^6(W, Y) \text{ or } \mathcal{V}_c^7(W, Z). \tag{26}$$

It is easily checked, that this leads to

$$\mathcal{W} = \mathcal{V}_c(b) = \mathcal{V}_c^7(Z, X) \text{ or } \mathcal{V}_c^6(X, Z) \text{ or } \mathcal{V}_c^6(W, Z). \tag{27}$$

All three vts are in (L). □

Proof of Theorem 2: We have to show: A tiling $\mathcal{T}$ is an infl_c-tiling if and only if it is an lmr_{vic}-tiling.

If $\mathcal{T}$ is a member of the inflation species, then by definition all its vts are in lmr_{vic} .

If on the other hand $\mathcal{T}$ satisfies lmr_{vic} and $\mathcal{L}$ is any cluster of $\mathcal{T}$, we have to prove:

There exists a prototile T and an exponent n, such that $\mathrm{infl}_c^n(T)$ contains a cluster which equals $\mathcal{L}$ (cf. [10]) on page 12).

Indeed: We only need to apply Remark 11 m times, such that $\sqrt{\tau}^{-m}\mathcal{L}$ is contained in a circular disc $\mathcal{D}$ of radius $.3$. Then, due to (8) $\mathcal{D}$ is contained in some vts $\mathcal{V}_c(x)$ of $\mathrm{DEFL}_c^m(\mathcal{T})$, which by Remark 11 is a member of lmr_{vic}.

By Definition 1 there is a prototile T and an exponent k such that a copy of $\mathcal{V}_c(x)$ is contained in $\mathrm{infl}_c^k(T)$ [12)]. Thus there is an isometry φ with

$$\varphi(\mathcal{L}) \subset \varphi(\mathcal{D}) \subset \mathrm{infl}_c^{k+m}(T).$$

□

6 Projecting the tilings of the species

As one of our aims is to calculate the FOURIER transform of the autocorrelation function of the vertex set of a $\sqrt{-\tau}$-tiling, we do not actually present a projection scheme for such a tiling but for the vertex set of such an tiling. From this vertex set, the tiling can be generated by the following method: The minimal distance of two vertices is τ^{-1}, and this solely occurs between a pair of vertex stars $\mathcal{V}^1$. So in this first step we can decorate all areas of rectangles $\mathcal{R}^1$ with the proper tiles. For the second step we have a closer look at the next larger possible distance, which is $\sqrt{\tau}^{-1}$. If none of both involved vertex stars is a $\mathcal{V}^1$, then both have to be $\mathcal{V}^2$, and with that we get all tiles lying in some $\mathcal{R}^2$. In the third step we use, that a similar fact is true for distance 1 of two vertex points: If none of both is known to be $\mathcal{V}^1$ or $\mathcal{V}^2$, then both are $\mathcal{V}^3$ and therefore all tiles in rectangulars $\mathcal{R}^3$ are known. As all small triangles have their rectangular vertex in a vertex $\mathcal{V}^1$ or $\mathcal{V}^3$ we already reconstructed all small triangles. These uniquely define supertiles of first order respectively all large triangles in such supertiles. Now the remaining unknown areas could only be single large triangles and pairs of large triangles. The dissection of these pairs into two large triangles is unique, because the splitting diagonal is restricted to one of the four orientations of edges in the tiling.

[12]) In fact we see from Figure 9: Every $\mathcal{V}_c^j(X,Z)$, and every $\mathcal{V}_c^j(Z,X)$ as well, occurs in $\mathrm{infl}_c^{j+3}(V)$. Hence $k=10$ will do.

6.1 A setting for defining the species by a strip projection method

A general scheme for a strip projection method can be seen in the following diagram [13]),

$$\begin{array}{ccccccc}
V & \subset & Z & & \subset & \mathbb{E}_P & \\
\Big\downarrow \pi^* & & \Big\downarrow \pi^* & \uparrow \pi_P & & \uparrow \pi_P & \\
& & & \Lambda & \subset & \mathbb{E}_S = \mathbb{E}_P \times \mathbb{E}_I & \\
& & & \downarrow \pi_I & & \downarrow \pi_I & \\
W & \subset & \mathbb{E}_I & & = & \mathbb{E}_I &
\end{array} \qquad (28)$$

where

- V is a discrete point set, here the vertex set of one of our tilings,
- Z is a $\mathbb{Z}$-module containing all vertices,
- $\mathbb{E}_P$ is the so-called *physical space*, the space the tiling lives in, the Euclidean plane in our case,
- $\mathbb{E}_I$ is the so-called *internal space*, its dimension is chosen as small as possible allowing a lattice Λ in the direct product $\mathbb{E}_S = \mathbb{E}_P \times \mathbb{E}_I$ (the so-called *superspace*) such that the projection π_P from $\mathbb{E}_S$ to $\mathbb{E}_P$, when restiricted to Λ, becomes a bijection from Λ to Z,
- π_I is the other projection from the $\mathbb{E}_S$ to $\mathbb{E}_I$ and we require $\pi_I(\Lambda)$ to be dense in $\mathbb{E}_I$,
- $\pi^* := \pi_I \circ \pi_P^{-1}$ is defined on Z and
- the *window* W is chosen such that $V = \{x \in Z \mid \pi^*(x) \in W\}$. We require W to be compact, the closure of its interior and that there are no projections of lattice points on the boundary of the window, $\partial W \cap \pi_I(\Lambda) = \emptyset$.

For a fixed lattice Λ and shape $W \subset \mathbb{E}_I$ one usually considers all windows $W + c$ ($c \in \mathbb{E}_I$), such that $\partial(W + c) \cap \pi_I(\Lambda) = \emptyset$.

Definition 5: *Given $\mathbb{E}_P$, $\mathbb{E}_I$, a lattice $\Lambda \in \mathbb{E}_P \times \mathbb{E}_I$ and a window W we call $c \in \mathbb{E}_I$* regular *if $\partial(W + c) \cap \pi_I(\Lambda) = \emptyset$ and denote with C the set of all regular c. For each regular c we define the projection set $V(c) := \{z \in Z \mid \pi^*(z) \in W + c\}$ and the set of all projection sets $\boldsymbol{P}(\Lambda, W) := \{V(c) \mid c \in C\}$.*

[13]) To be honest, this is not the most general scheme, as the physical and internal spaces need not to be Euclidean ones, they only have to be topological Abelian groups; the lattice Λ then becomes a discrete subgroup of the direct product (compare [13]).

We will find the correct terms for the vertex sets of our tilings in two steps: first we derive the $\mathbb{Z}$-module Z and choose a matching internal space and lattice. In a second step we choose a proper window. In this subsection we will describe how we get to these different sets by smart guessing and choosing without bothering about proofs. In the next subsection we will proof the whole setting at once.

A closer look at the tilings of the species suggests, that all vertices lie in the rank four $\mathbb{Z}$-module $Z := (\sqrt{\tau}\,\langle 1,\tau\rangle) \times \langle 1,\tau\rangle$ (at least if one vertex is at the origin). So it suggests itself to take as superspace $\mathbb{E}_S^4 = \mathbb{E}_P^2 \times \mathbb{E}_I^2$. Let π_P be the projection on the first two components and π_I the projection on the last two components of a vector $x \in \mathbb{E}_S^4$. To find a possible basis $\{l_1, l_2, l_3, l_4\}$ of the matching lattice $\Lambda \subset E_S^4$ we split the inflation infl as presented in Section 1 into two parts: the scaling (and rotation) given by the linear map β and the subdivision or (as we only look at the vertex set in this section) the addition of new vertices σ. Like the module Z is invariant under the action of β, the lattice Λ should be invariant under the lifted version β_S of β. That is, β_S has to be an uni-modular transformation of Λ. β_S, the lift of β on Λ, is defined as $\beta_S = \beta \times \beta^* = \beta \times (\pi^* \circ \beta \circ {\pi^*}^{-1})$. As $\beta(\binom{0}{1}) = \binom{-\sqrt{\tau}}{0}$, $\beta(\binom{-\sqrt{\tau}}{0}) = \binom{0}{-\tau}$, $\beta(\binom{0}{-\tau}) = \binom{\sqrt{\tau}^3}{0}$ and $\beta(\binom{\sqrt{\tau}^3}{0}) = \binom{0}{1} - \binom{0}{-\tau}$, with $\pi_P(l_1) := \binom{0}{1}$, $\pi_P(l_2) := \binom{-\sqrt{\tau}}{0}$, $\pi_P(l_3) := \binom{0}{-\tau}$, $\pi_P(l_4) := \binom{\sqrt{\tau}^3}{0}$ β_S becomes the uni-modular transformation which maps $l_1 \mapsto l_2 \mapsto l_3 \mapsto l_4 \mapsto l_1 - l_3$. Taking β_S as a linear map on $\mathbb{R}^4$ the eigenvalues are $\pm\sqrt{-\tau}$ and $\pm\sqrt{\tau}^{-1}$ and $\mathbb{E}_P^2$ is the real part of the sum of the eigenspaces to $\pm\sqrt{-\tau}$. As this is characteristic for the lift of the expansion map β, the linear inflation factor is indeed rather $\sqrt{-\tau}$ than $\sqrt{\tau}$. To make the projection fit to the inflation, the last components of the lattice basis have to be chosen in such a way, that $\mathbb{E}_I^2$ contains the eigenspaces to the other two eigenvalues. Because it makes later calculations more convenient we choose β^* to be represented by the matrix $\begin{pmatrix} 0 & \sqrt{\tau}^{-1} \\ \sqrt{\tau}^{-1} & 0 \end{pmatrix}$ and $\pi_I(l_1) = \binom{-\sqrt{\tau}^3}{1}$. With this choice the lattice Λ reads

$$\Lambda = \langle l_1, l_2, l_3, l_4 \rangle = \left\langle \begin{pmatrix} 0 \\ 1 \\ -\sqrt{\tau}^3 \\ 1 \end{pmatrix}, \begin{pmatrix} -\sqrt{\tau} \\ 0 \\ \sqrt{\tau}^{-1} \\ -\tau \end{pmatrix}, \begin{pmatrix} 0 \\ -\tau \\ -\sqrt{\tau} \\ \tau^{-1} \end{pmatrix}, \begin{pmatrix} \sqrt{\tau}^3 \\ 0 \\ \sqrt{\tau}^{-3} \\ -1 \end{pmatrix} \right\rangle. \qquad (29)$$

To get an idea of how the window W may look like, we take some points of Λ and project them into $\mathbb{E}_I^2$, distinguishing between points which belong to a certain tiling and points which do not. In Figure 15 every filled circle corresponds to a vertex of the tiling indicated in Figure 10 (if the origin is settled at the vertex denoted with $\mathcal{V}^6(X,Z)$), whereas every unfilled circle represents a lattice point not being projected on a vertex of that tiling. Looking at this figure, we claim, that the window $W + c$ is a rectangular box with edge length $2\sqrt{\tau}^3$ and 2τ which is translated by some vector c. So we define $W := \square(\binom{-\sqrt{\tau}^3}{-\tau}, \binom{\sqrt{\tau}^3}{\tau})$, denoting by $\square(\binom{x_1}{x_2}, \binom{y_1}{y_2})$ the closed rectangular set with lower left corner $\binom{x_1}{x_2}$ and upper right corner $\binom{y_1}{y_2}$, $\square(\binom{x_1}{x_2}, \binom{y_1}{y_2}) := [x_1, y_1] \times [x_2, y_2]$. For $a, b \in \mathbb{Z}$ every line $\binom{\mathbb{R}}{a+b\tau}$ and $\binom{a\sqrt{\tau}+b\sqrt{\tau}^3}{\mathbb{R}}$ in $\mathbb{E}_I^2$ contains a dense set of lattice points projected by π_I, but every other horizontal or vertical line contains no points of $\pi_I(\Lambda)$. Hence the set

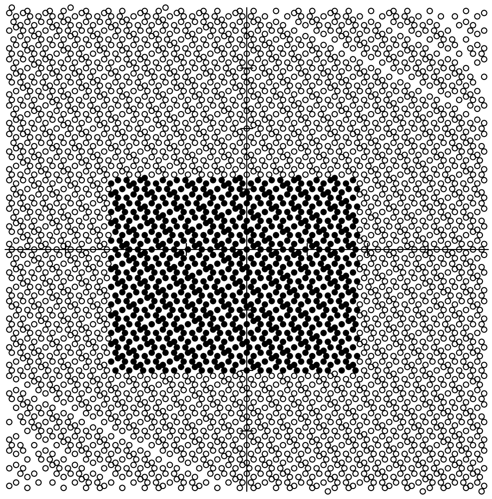

Figure 15: Determining the window experimentally

C of all regular points c is given by

$$C = \mathbb{E}_I^2 \setminus \bigcup_{a,b\in\mathbb{Z}} \left(\begin{pmatrix} \mathbb{R} \\ a+b\tau \end{pmatrix} \cup \begin{pmatrix} a\sqrt{\tau}+b\sqrt{\tau}^3 \\ \mathbb{R} \end{pmatrix} \right), \tag{30}$$

because $c \in \bigcup \begin{pmatrix} \mathbb{R} \\ a+b\tau \end{pmatrix}$ if and only if $c + \begin{pmatrix} [-\sqrt{\tau}^3, \sqrt{\tau}^3] \\ \pm\tau \end{pmatrix} \subset \bigcup \begin{pmatrix} \mathbb{R} \\ a+b\tau \end{pmatrix}$ and similar for the vertical lines. Using this terms we state

Theorem 3: *For every regular* c*, the above projection set* $V(c) = \{z \in Z \mid \pi^*(z) \in W + c\}$ *is the vertex set* $V(\mathcal{P})$ *of a tiling* $\mathcal{P} \in \boldsymbol{\mathcal{S}}(\mathfrak{F}, \mathrm{infl})$*, the inflation species of Definition 1.*

6.2 Proof of Theorem 3

The tiles A and X occur in a tiling $\mathcal{P} \in \boldsymbol{\mathcal{S}}(\mathfrak{F}, \mathrm{lmr}_{vi})$ in (at most) four orientations given by the four linear maps $\varphi_0 = \mathrm{id}$, the reflections φ_1 and φ_2 defined in Section 2 and the composition of both reflections, the $180°$ rotation φ_3. The maps φ_i^* corresponding to φ_i in $\mathbb{E}_I^2$ (the linear extension of $\pi^* \circ \varphi_i \circ {\pi^*}^{-1}$ on $\pi_I(\Lambda)$ to $\mathbb{E}_I^2$) are $\varphi_0^* = \mathrm{id}$, φ_1^* and φ_2^* are the reflections at the vertical respectively horizontal line and φ_3^* is of course again the $180°$ rotation.

We now split the window W into 24 parts $W_{i,j}$ $(i = 1, \ldots, 6,\ \ j = 0, \ldots, 3)$ given by $W_{1,0} = \square\left(\begin{pmatrix} \sqrt{\tau} \\ 0 \end{pmatrix}, \begin{pmatrix} \sqrt{\tau}^3 \\ \tau \end{pmatrix}\right)$, $W_{2,0} = \square\left(\begin{pmatrix} 0 \\ 1 \end{pmatrix}, \begin{pmatrix} \sqrt{\tau} \\ \tau \end{pmatrix}\right)$, $W_{3,0} = \square\left(\begin{pmatrix} \sqrt{\tau}^{-1} \\ 0 \end{pmatrix}, \begin{pmatrix} \sqrt{\tau} \\ 1 \end{pmatrix}\right)$, $W_{4,0} = \square\left(\begin{pmatrix} 0 \\ \tau^{-1} \end{pmatrix}, \begin{pmatrix} \sqrt{\tau}^{-1} \\ 1 \end{pmatrix}\right)$, $W_{5,0} = \square\left(\begin{pmatrix} \sqrt{\tau}^{-3} \\ 0 \end{pmatrix}, \begin{pmatrix} \sqrt{\tau}^{-1} \\ \tau^{-1} \end{pmatrix}\right)$, $W_{6,0} = \square\left(\begin{pmatrix} 0 \\ 0 \end{pmatrix}, \begin{pmatrix} \sqrt{\tau}^{-3} \\ \tau^{-1} \end{pmatrix}\right)$ and $W_{i,j} = \varphi_j^*(W_{i,0})$. (The $W_{i,0}$ are the black boxes in the last column of Table 1.) $c \in C$ ensures, that the boundary $\partial W_{i,j}$ of each $W_{i,j}$ contains no points of $\pi^*(Z)$. So we uniquely can assign to every point $x \in V(c)$ a vertex star $\mathcal{V}^i$ and an orientation φ_j according to $\pi^*(x) \in W_{i,j}$.

Table 1 then shows (explicitly for $j = 0$, but for the other orientations the situation is of course congruent), that if vertex star $\mathcal{V}^i$ and orientation φ_j is assigned to $x \in V(c)$, then

No. (i)	Vertex stars $\mathcal{V}^i$	Image of the vertex points under π^*	possible positions in W (■ $= W_{i,0}$)
1	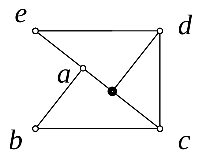	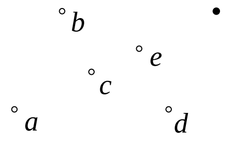	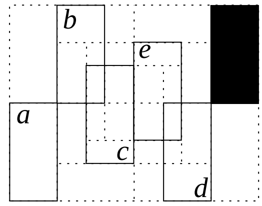
2	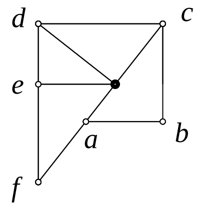	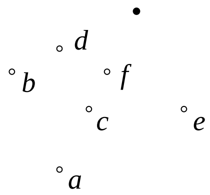	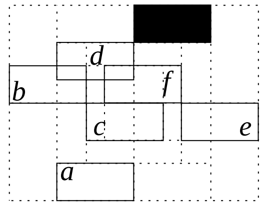
3	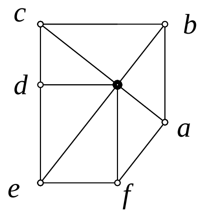	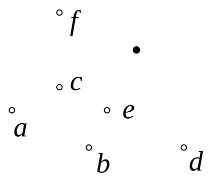	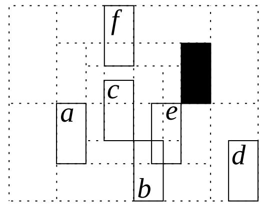
4	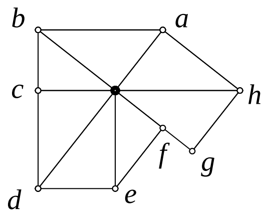	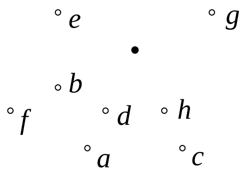	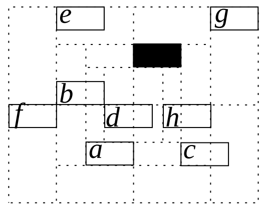
5	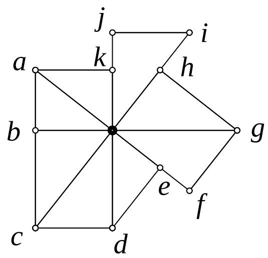	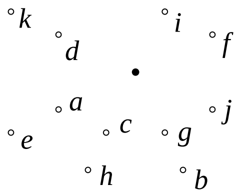	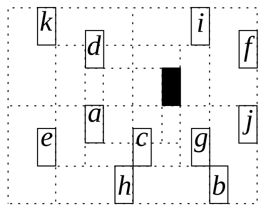
6	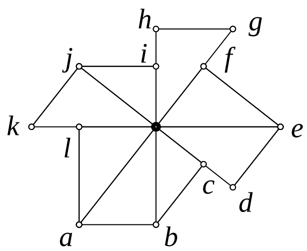	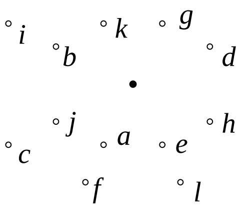	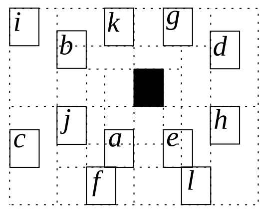

Table 1: Internal images of the vertex stars

$V(c)$ contains all vertex points of the tiles in the vertex star $\varphi_j(\mathcal{V}^i)+x$: For the vertex stars in column 2, column 3 shows the position of the internal images of the vertices of all tiles relative to the point where the vertex star is settled. The last column then proofs, that if $x \in W_{i,j}$, all these internal images are in the window W.

Furthermore, by investigating the possible positions of the points $a, \ldots$ in the window W, one easily sees, that to each of those points such a vertex star and orientation is assigned, that its correctly oriented vertex star fits together with the central one, i.e. the intersection consists of non overlapping tiles.

So starting from one point $x \in V(c)$ it is possible to find tiles surrounding x, such that every vertex of these tiles is a point of $V(c)$, and then to find tiles surrounding all these vertices with the same property and so on. Finally one gets a tiling $\mathcal{P}_{c,x} \in \boldsymbol{\mathcal{S}}(\mathfrak{F}, \mathrm{lmr}_{vi})$, whose vertex set $V(\mathcal{P}_{c,x})$ is contained in $V(c)$.

The same can be done for another $y \in V(c)$ leading to $\mathcal{P}_{c,y} \in \boldsymbol{\mathcal{S}}(\mathfrak{F}, \mathrm{lmr}_{vi})$. The determination of the vertex star and the orientation assigned to a point $y \in V(c)$ is unique. Hence it is $V(\mathcal{P}_{c,x}) = V(\mathcal{P}_{c,y})$ for $y \in V(\mathcal{P}_{c,x})$ and $V(\mathcal{P}_{c,x}) \cap V(\mathcal{P}_{c,y}) = \emptyset$ for $y \in V(c) \setminus V(\mathcal{P}_{c,x})$. Therefore

$$V(c) = \,.\!\!\bigcup_{x \in X} V(\mathcal{P}_{c,x}) \tag{31}$$

for some $X \subset V(c)$ and $\mathcal{P}_{c,x} \in \boldsymbol{\mathcal{S}}(\mathfrak{F}, \mathrm{lmr}_{vi})$.

The global density

$$\mathrm{dens}(V(c)) := \lim_{r\to\infty} \frac{\#(V(c) \cup (r\mathbb{B}^d + x))}{\mathrm{Vol}(r\mathbb{B}^d)} \tag{32}$$

($x \in \mathbb{E}^2_P$) exists for the projection set $V(c)$ (independent of $x \in \mathbb{E}^2_P$ and $c \in C$) and is given by

$$\mathrm{dens}(V(c)) = \frac{\mathrm{Vol}(W)}{\det(\Lambda)}. \tag{33}$$

(For a rather general proof of this existence and formula see [13].) Hence

$$\mathrm{dens}(V(c)) = \frac{4\sqrt{\tau}^5}{10\tau} = \frac{2}{5}\sqrt{\tau}^3 \approx .82327 \quad . \tag{34}$$

The global density of a set $V(\mathcal{P})$, $\mathcal{P} \in \boldsymbol{\mathcal{S}}(\mathfrak{F}, \mathrm{lmr}_{vi})$ can be estimated by

$$\inf_{x \in \mathbb{E}^2_P} \liminf_{r\to\infty} \frac{\#(V(\mathcal{P}) \cup (r\mathbb{B}^d + x))}{\mathrm{Vol}(r\mathbb{B}^d)} \geq \frac{1}{2} \cdot \frac{1}{\mathrm{Vol}(X)} = \sqrt{\tau}^{-3} \approx .48587 \tag{35}$$

and

$$\sup_{x \in \mathbb{E}^2_P} \limsup_{r\to\infty} \frac{\#(V(\mathcal{P}) \cup (r\mathbb{B}^d + x))}{\mathrm{Vol}(r\mathbb{B}^d)} \leq 1 \cdot \frac{1}{\mathrm{Vol}(X)} = 2\sqrt{\tau}^{-3} \approx .97174 \tag{36}$$

as $\frac{1}{2} \cdot \frac{1}{\mathrm{Vol}(X)}$ is the density of vertex points in a triangle X with no vertices on edges and therefore the smallest possible local density in a tile, and $1 \cdot \frac{1}{\mathrm{Vol}(X)}$ is the density of vertex points in a triangle X with vertices on both possible edges and therefore the largest possible local density in a tile. (The vertex density in a triangle A is always $\frac{1}{2} \cdot \frac{1}{\mathrm{Vol}(A)} = \sqrt{\tau}^{-1} \approx .786$ in-between.)

A comparison of (35) and (36) with (34) shows that the union in (31) is a union over just one tiling, that is to say

$$\left.\begin{array}{l}\text{for every } V(c) \in \boldsymbol{P}(\Lambda, W) \text{ there is a (uniquely defined) } \mathcal{P}_c \in \boldsymbol{\mathcal{S}}(\mathfrak{F}, \mathrm{lmr}_{vi}), \\ \text{such that } V(c) = V(\mathcal{P}_c). \end{array}\right\} \tag{37}$$

For each $c \in C$ let in the remainder $\mathcal{P}_c$ be that uniquely defined tiling in $\boldsymbol{\mathcal{S}}(\mathfrak{F}, \mathrm{lmr}_{vi})$ with $V(\mathcal{P}_c) = V(c)$. In order to show that every $\mathcal{P}_c$ is in fact a tiling in $\boldsymbol{\mathcal{S}}(\mathfrak{F}, \mathrm{infl})$, we define an inflation on $\boldsymbol{P}(\Lambda, W)$ by $\mathrm{infl}(V(c)) := V(\mathrm{infl}(\mathcal{P}_c))$ and describe this map in terms of the internal space. This is done separately for both parts of the inflation $\mathrm{infl} = \sigma \circ \beta$ (cf. Section 6.1). We already have the internal counterpart β^* to β for which

$$\begin{aligned} V(\beta(\mathcal{P}_c)) = \beta(V(\mathcal{P}_c)) = \beta(V(c)) &= \{\beta(x) \in Z \mid \pi^*(x) \in W + c\} \\ &= \{x \in Z \mid \pi^*(x) \in \beta^*(W + c)\} \end{aligned} \tag{38}$$

holds. The definition of the inflation infl (cf. Fig. 1) shows, that the subdivision σ only produces new vertex points in a tiling $\beta(\mathcal{P}_c)$ on the long edge of a tile $\beta(X)$. And even that only occurs if two such edges meet edge to edge, that means only in a scaled rectangle “0” (cf. Fig. 4). Furthermore, from the vertex stars $\mathcal{V}^1, \ldots, \mathcal{V}^6$ it can be revealed, that four vertex points in such a rectangular position uniquely determine a scaled rectangle “0”. So for the scaled vertex set $\beta(V(c)) = \beta(V(\mathcal{P}_c))$ all new vertices can be described in the form $(\beta(V(c)) + t_{1,j}) \cap (\beta(V(c)) + t_{2,j}) \cap (\beta(V(c)) + t_{3,j}) \cap (\beta(V(c)) + t_{4,j})$, where $t_{i,0}$ are the translations, which move the four points of a scaled rectangle “0” in orientation φ_0 into one of the two new vertices inside and $t_{i,j} = \varphi_j(t_{i,0})$. Fixing the orientation of a scaled rectangle “0” as that of vertex star $\mathcal{V}^1$ we get $t_{1,0} = \begin{pmatrix}\sqrt{\tau} \\ -1\end{pmatrix}$, $t_{2,0} = \begin{pmatrix}\sqrt{\tau} \\ \tau^{-1}\end{pmatrix}$, $t_{3,0} = \begin{pmatrix}-\sqrt{\tau}^{-1} \\ -1\end{pmatrix}$, $t_{4,0} = \begin{pmatrix}-\sqrt{\tau}^{-1} \\ \tau^{-1}\end{pmatrix}$ the other $t_{i,j}$ by $t_{i,j} = \varphi_j(t_{i,0})$. Hence the inflation of $V(c)$ as a pure point operation reads

$$\mathrm{infl}(V(c)) = \sigma\left(\beta(V(c))\right) \tag{39}$$

$$= \beta(V(c)) \cup \bigcup_{j \in \{0,\ldots,3\}} \left(\bigcap_{i \in \{1,\ldots,4\}} (\beta(V(c)) + t_{i,j}) \right). \tag{40}$$

Using the notation $t^*_{i,j} = \pi^*(t_{i,j})$ (which is well defined as all $t_{i,j} \in Z$) we define for $W' \subset \mathbb{E}^2_I$

$$\sigma^*(W') := W' \cup \bigcup_{j \in \{0,\ldots,3\}} \left(\bigcap_{i \in \{1,\ldots,4\}} (W' + t^*_{i,j}) \right). \tag{41}$$

With this σ^* we have the equivalence

$$x \in \sigma(\beta(V(c))) \Leftrightarrow \pi^*(x) \in \sigma^*(\beta^*(W + c)) \tag{42}$$

respectively

$$\operatorname{infl}(V(c)) = \{z \in Z \mid \pi^*(z) \in \operatorname{infl}^*(W + c)\} \tag{43}$$

where $\operatorname{infl}^* := \sigma^* \circ \beta^*$.

Deriving $t^*_{1,0} = \begin{pmatrix}\sqrt{\tau}\\ \tau^{-1}\end{pmatrix}$, $t^*_{2,0} = \begin{pmatrix}2\sqrt{\tau}\\ 0\end{pmatrix}$, $t^*_{3,0} = \begin{pmatrix}\sqrt{\tau}^{-1}\\ \tau\end{pmatrix}$ and $t^*_{4,0} = \begin{pmatrix}\sqrt{\tau}^{3}\\ 1\end{pmatrix}$ and using $\beta^*(W + c) = \beta^*(W) + \beta^*(c) = \square\left(\begin{pmatrix}-\sqrt{\tau}\\ -\tau\end{pmatrix}, \begin{pmatrix}\sqrt{\tau}\\ \tau\end{pmatrix}\right) + \beta^*(c)$ the "φ_0" component in the union of σ^* applied to $\beta^*(W + c)$ reads

$$\begin{aligned}
&\bigcap_{i\in\{1,\ldots,4\}} (\beta^*(W + c) + t^*_{i,0}) \\
&= \left(\square\left(\begin{pmatrix}0\\ -1\end{pmatrix}, \begin{pmatrix}2\sqrt{\tau}\\ 2\tau-1\end{pmatrix}\right) \cap \square\left(\begin{pmatrix}\sqrt{\tau}\\ -\tau\end{pmatrix}, \begin{pmatrix}3\sqrt{\tau}\\ \tau\end{pmatrix}\right) \cap \square\left(\begin{pmatrix}-\sqrt{\tau}^{-3}\\ 0\end{pmatrix}, \begin{pmatrix}\sqrt{\tau}^{3}\\ 2\tau\end{pmatrix}\right) \cap \square\left(\begin{pmatrix}\sqrt{\tau}^{-1}\\ -\tau^{-1}\end{pmatrix}, \begin{pmatrix}\sqrt{\tau}^{5}\\ \tau^{2}\end{pmatrix}\right)\right) + \beta^*(c) \\
&= \square\left(\begin{pmatrix}\sqrt{\tau}\\ 0\end{pmatrix}, \begin{pmatrix}\sqrt{\tau}^{3}\\ \tau\end{pmatrix}\right) + \beta^*(c)
\end{aligned} \tag{44}$$

(compare Fig. 16). This is exactly $W_{1,0} + c$, which is not to surprising, as $\mathcal{V}^1$ arises during inflation only as result of two tiles X sharing the long edge. Because of the symmetry of the

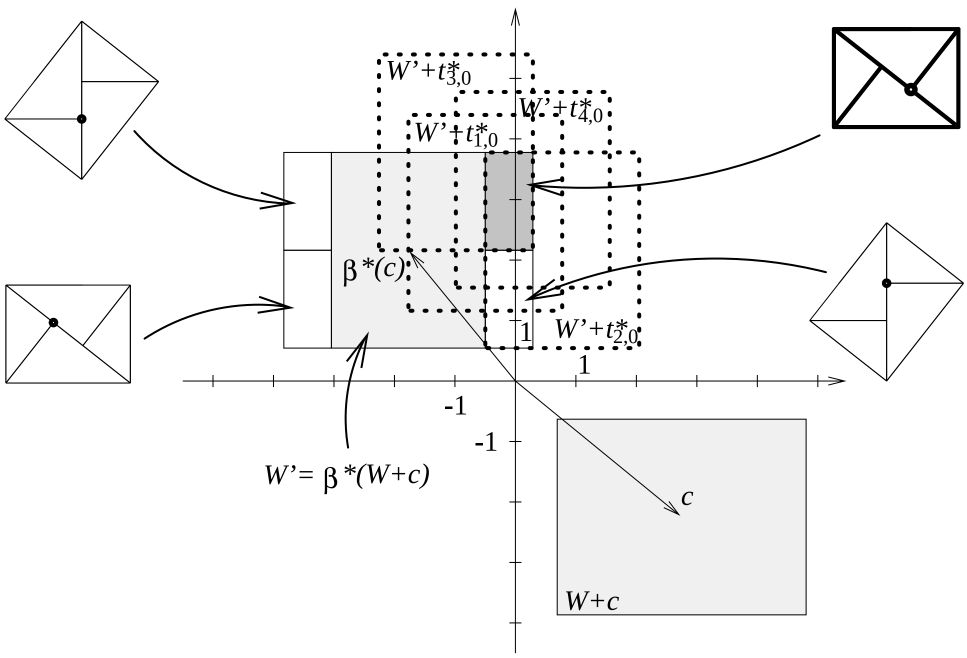

Figure 16: "Inflation" of the window $W + c$

$t_{i,j}$, the other components of (41) have to be $\varphi_j(W_{1,0}) + c = W_{1,j} + c$ and the "inflation" of a window $W + c$ simplifies to

$$\operatorname{infl}^*(W + c) = \sigma^*(\beta^*(W + c)) = (\beta^*(W) \cup W_{1,0} \cup W_{1,1} \cup W_{1,2} \cup W_{1,3}) + \beta^*(c) = W + \beta^*(c). \tag{45}$$

So finally we have a very simple description of the inflation of a projection set $\mathrm{infl}(V(c)) = \mathrm{infl}(V(\mathcal{P}_c)) = V(\mathrm{infl}(\mathcal{P}_c))$ in terms of the internal space

$$\mathrm{infl}(V(c)) = V(\beta^*(c)). \tag{46}$$

As $\beta^*(\mathbb{E}_I \setminus C) = \mathbb{E}_I \setminus C$ and β^* is bijective we have, that this inflation infl is a bijection of $\boldsymbol{P}(\Lambda, W)$ into itself. Hence $\mathrm{defl} = \mathrm{infl}^{-1}$ exists and reads $\mathrm{defl}(V(c) = V({\beta^*}^{-1}(c))$.

As the deflation of a tiling is uniquely defined depending locally only on neighbouring tiles (compare Remark 1), for $\mathcal{P} \in \boldsymbol{\mathcal{S}}(\mathfrak{F}, \mathrm{lmr}_{vi})$ $\mathrm{defl}(\mathcal{P})$ is well defined, even though it might be, that $\mathrm{defl}(\mathcal{P})$ is no longer a member of $\boldsymbol{\mathcal{S}}(\mathfrak{F}, \mathrm{lmr}_{vi})$. But for a $\mathcal{P}_c \in \boldsymbol{\mathcal{S}}(\mathfrak{F}, \mathrm{lmr}_{vi})$ we can state

$$V(\mathrm{defl}(\mathcal{P}_c)) = \mathrm{defl}(V(c)) = V({\beta^*}^{-1}(c)) = V(\mathcal{P}_{{\beta^*}^{-1}(c)}) \tag{47}$$

and as the vertex set $V(\mathcal{P}_{{\beta^*}^{-1}(c)})$ uniquely defines the tiling $\mathcal{P}_{{\beta^*}^{-1}(c)} \in \boldsymbol{\mathcal{S}}(\mathfrak{F}, \mathrm{lmr}_{vi})$ with $\mathrm{infl}(\mathcal{P}_{{\beta^*}^{-1}(c)}) = \mathcal{P}_c$, we find $\mathrm{defl}(\mathcal{P}_c) = \mathcal{P}_{{\beta^*}^{-1}(c)} \in \boldsymbol{\mathcal{S}}(\mathfrak{F}, \mathrm{lmr}_{vi})$. Therefore the deflation can be iterated on the the set $\{\mathcal{P}_c \mid c \in C\}$.

For a tiling $\mathcal{P}_c$ ($c \in C$) a cluster $\mathcal{C} \subset \mathcal{P}_c$ is covered by a ball of some radius ρ. If n is chosen such that $\frac{1}{2}\tau^{-1} \cdot \sqrt{\tau}^{\,n} > \rho$ we can conclude that $\mathcal{C}$ is part of the nth inflation of a vertex star of $\mathrm{defl}^n(\mathcal{P}_c)$ (compare (8)). Each vertex star is contained in the tenth inflation of some tile A (compare proof of Remark 3a respectively Fig. 10), hence $\mathcal{C}$ is congruent to some part of $\mathrm{infl}^{n+10}(A)$. As this is true for each cluster of $\mathcal{P}_c$, according to Definition 1 $\mathcal{P}_c$ is a member of $\boldsymbol{\mathcal{S}}(\mathfrak{F}, \mathrm{infl})$. □

6.3 On the converse of Theorem 3

While Theorem 3 states

$$\boldsymbol{P}(\Lambda, W) \subset \{V(\mathcal{P}) \mid \mathcal{P} \in \boldsymbol{\mathcal{S}}(\mathfrak{F}, \mathrm{infl})\} \tag{48}$$

the converse is obviously not true. Despite of all $V(c) \subset Z$, the vertices of $\mathcal{P} \in \boldsymbol{\mathcal{S}}(\mathfrak{F}, \mathrm{infl})$ can be in arbitrary positions, and while each triangle reconstructed from a $V(c)$ is in one of the orientations $\varphi_0, \ldots, \varphi_3$, with one tiling $\mathcal{P} \in \boldsymbol{\mathcal{S}}(\mathfrak{F}, \mathrm{infl})$, all congruent copies of $\mathcal{P}$ are also members of $\boldsymbol{\mathcal{S}}(\mathfrak{F}, \mathrm{infl})$. But besides these trivial cases there are some *singular* tilings $\mathcal{P} \in \boldsymbol{\mathcal{S}}(\mathfrak{F}, \mathrm{infl})$ with $V(\mathcal{P}) \subset Z$ and all triangles nicely oriented, whose vertex set is not a projection set in $\boldsymbol{P}(W, \Lambda)$. To construct an example, we take a tiling $\mathcal{P}_c$ with $c \in C \cap (-W_{6,0})$. Then $0 \in V(\mathcal{P}_c)$ and $\mathcal{V}(0) = \mathcal{V}^6$ in orientation φ_0. Now we define $\mathcal{P} := \lim \mathrm{infl}^n(\mathcal{P}_0)$ for $n \to \infty$ (cf. Fig. 17). $\mathcal{P}$ is well-defined as $\mathcal{V}^6 \subset \mathrm{infl}(\mathcal{V}^6)$. Obviously $\mathcal{P}$ is a member of $\boldsymbol{\mathcal{S}}(\mathfrak{F}, \mathrm{infl})$, but $V(\mathcal{P}) \notin \boldsymbol{P}(\Lambda, W)$, because $V(\mathrm{infl}^n(\mathcal{P}_c)) = V(\beta^{*n}(c))$ and $\lim \beta^{*n}(c) = 0 \notin C$. Nevertheless

$$\overline{\boldsymbol{P}(\Lambda, W)} = \left\{ V(\mathcal{P}) \;\middle|\; \begin{array}{l} \mathcal{P} \in \boldsymbol{\mathcal{S}}(\mathfrak{F}, \mathrm{infl}),\ V(\mathcal{P}) \subset Z \text{ and all } T \in \mathcal{P} \text{ are} \\ \text{in orientation } \varphi_0,\ \varphi_1,\ \varphi_2 \text{ or } \varphi_3 \end{array} \right\} \tag{49}$$

with one of the usual topologies in the space of all discrete subsets of $\mathbb{E}^2$ defined by identity around the origin (cf. for example [6]).

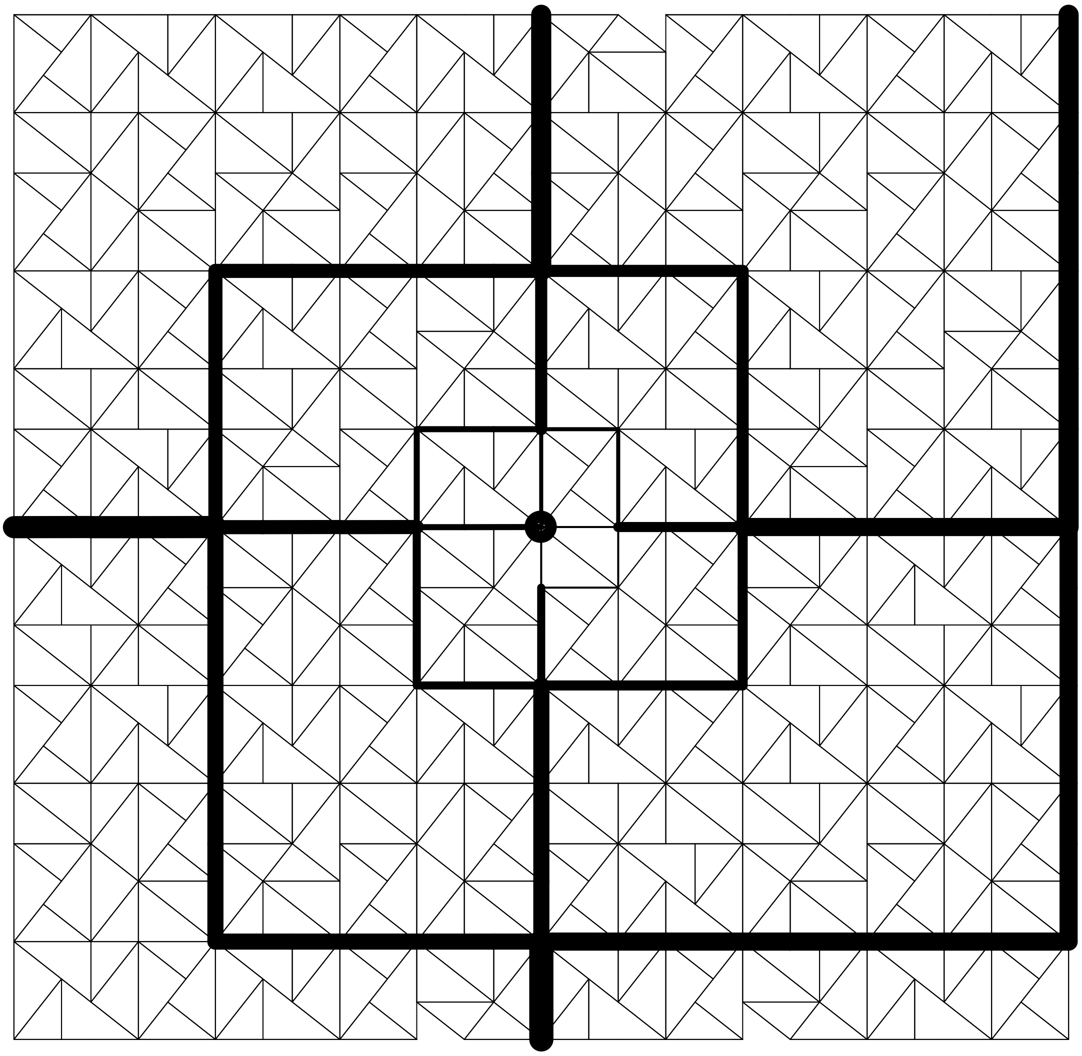

Figure 17: An inflation invariant tiling

6.4 *Non equivalence to the* Ammann *tiling* $\boldsymbol{\mathcal{S}}_{A2}$

Obviously the tiling $\mathcal{P}$ of the last subsection is invariant under inflation. Together with the rotational part of the expansion map β this causes an infinite spirale in the center of the tiling, see Figure 17. Now the repetitivity of the species enforces every local part of every tiling to contain finite spirals. Similar spirals can be observed in another species of tilings. The connection to this species will be investigated in this subsection.

In [2] chapter 10.4 Grünbaum and Shephard describe a class A2 of species with so-called chair tiles designed by Robert Ammann. One of these species (choosing the free parameter to be τ) has an inflation with the real inflation factor $\sqrt{\tau}$, and a closer look shows that a precise description of the inflation again uses the expansion map β defined in Section 2. Let us denote with $\boldsymbol{\mathcal{S}}_{\mathsf{A2}}$ this special species of the whole class in the remainder.

The fact that $\boldsymbol{\mathcal{S}}(\mathfrak{F}, \mathrm{infl})$ has no local matching rule whereas $\boldsymbol{\mathcal{S}}_{\mathsf{A2}}$ has one, shows that the two species are not mutually locally derivable (MLD). (For a introduction into the equivalence concept MLD for LI-classes of tilings see [9].) We will give here another argument for this non equivalence, based on the projection of both species. In [5] was proven, that two projection sets projected from the same lattice are MLD, if and only if the window(s) of one projection set can be reassembled by a finite collection of the operations $A \cup B$, $\overline{(A \cap B)^\circ}$, $\overline{A \setminus B}$ applied to translates of the window(s) of the other projection set and vice versa.

In order to get a tiling $\boldsymbol{\mathcal{S}}_{\mathsf{A2}}$ by a projection of the lattice Λ (see (29)), we choose the edge lengths of S to be $\frac{1}{\sqrt{2}}\sqrt{\tau}^{-3}$, $\frac{1}{\sqrt{2}}\tau^{-1}$, $\frac{1}{\sqrt{2}}\sqrt{\tau}^{-1}$, $\frac{1}{\sqrt{2}}$, $\frac{1}{\sqrt{2}}\sqrt{\tau}$, $\frac{1}{\sqrt{2}}\tau$ and that of L to be $\frac{1}{\sqrt{2}}\tau^{-1}$, $\frac{1}{\sqrt{2}}\sqrt{\tau}^{-1}$, $\frac{1}{\sqrt{2}}$, $\frac{1}{\sqrt{2}}\sqrt{\tau}$, $\frac{1}{\sqrt{2}}\tau$ and $\frac{1}{\sqrt{2}}\sqrt{\tau}^{3}$, respectively.

The orientation of the two prototiles is fixed such that all edges are parallel to the reflection lines of φ_1 and φ_2 defined in Section 2 (cf. Fig 18). Then there are four orientations of the two tiles given by $S_i = \varphi_i(S)$ and $L_i = \varphi_i(L)$ with φ_i as in Section 6.2.

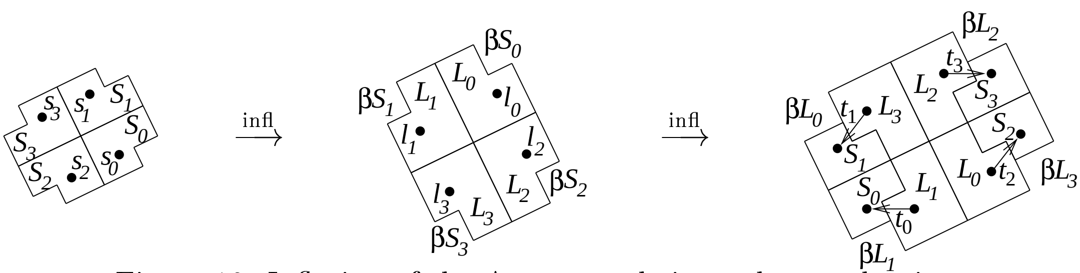

Figure 18: Inflation of the AMMANN chairs and control points

In contrast to Section 6 we will not project the vertices of a tiling of $\boldsymbol{\mathcal{S}}_{\mathsf{A2}}$ because the $\mathbb{Z}$-module defined by the vertices is — in contrast to the triangle tiling — not the limit translation module determining the projection. Therefore we choose certain control points, one class for each prototile in each orientation. As position of the control points we choose the center of a spiral built by consecutive supertiles. Given a tiling $\mathcal{P} \in \boldsymbol{\mathcal{S}}_{\mathsf{A2}}$ the sets $P_{T_i}(\mathcal{P})$ ($T = S, L$ and $i = 0, 1, 2, 3$) of all control points can be derived by putting a control point in each tile. Given all control point sets P_{T_i} one gets a tiling by surrounding each control point with the assigned tile.

The inflation of a system of control point sets of a tiling is of course defined as the system of control point sets of the inflated tiling. From Figure 18 we can read off

$$\begin{aligned}
P_{S_0}(\mathrm{infl}_{\boldsymbol{\mathcal{S}}_{\mathsf{A2}}}(\mathcal{P})) &= \beta(P_{L_1}(\mathcal{P})) + t_0 & P_{L_0}(\mathrm{infl}_{\boldsymbol{\mathcal{S}}_{\mathsf{A2}}}(\mathcal{P})) &= \beta(P_{S_0}) \cup \beta(P_{L_3}) \\
P_{S_1}(\mathrm{infl}_{\boldsymbol{\mathcal{S}}_{\mathsf{A2}}}(\mathcal{P})) &= \beta(P_{L_0}(\mathcal{P})) + t_1 & P_{L_1}(\mathrm{infl}_{\boldsymbol{\mathcal{S}}_{\mathsf{A2}}}(\mathcal{P})) &= \beta(P_{S_1}) \cup \beta(P_{L_1}) \\
P_{S_2}(\mathrm{infl}_{\boldsymbol{\mathcal{S}}_{\mathsf{A2}}}(\mathcal{P})) &= \beta(P_{L_3}(\mathcal{P})) + t_2 & P_{L_2}(\mathrm{infl}_{\boldsymbol{\mathcal{S}}_{\mathsf{A2}}}(\mathcal{P})) &= \beta(P_{S_2}) \cup \beta(P_{L_2}) \\
P_{S_3}(\mathrm{infl}_{\boldsymbol{\mathcal{S}}_{\mathsf{A2}}}(\mathcal{P})) &= \beta(P_{L_2}(\mathcal{P})) + t_3 & P_{L_3}(\mathrm{infl}_{\boldsymbol{\mathcal{S}}_{\mathsf{A2}}}(\mathcal{P})) &= \beta(P_{S_3}) \cup \beta(P_{L_0})
\end{aligned} \tag{50}$$

with $t_0 = \begin{pmatrix} -\sqrt{\tau}^{-1} \\ 0 \end{pmatrix}$, $t_1 = \begin{pmatrix} -\sqrt{\tau}^{-3} \\ -\tau^{-1} \end{pmatrix}$, $t_2 = \begin{pmatrix} \sqrt{\tau}^{-3} \\ \tau^{-1} \end{pmatrix}$ and $t_3 = \begin{pmatrix} \sqrt{\tau}^{-1} \\ 0 \end{pmatrix}$. Now the system of windows

(cf. Fig 19)

$$
\begin{array}{ll}
W_{S_0} = \triangle\left(\begin{pmatrix}-\sqrt{\tau}\\ \tau^2\end{pmatrix}, \begin{pmatrix}-\sqrt{\tau}^3\\ 1\end{pmatrix}, \begin{pmatrix}-\sqrt{\tau}^5\\ \tau\end{pmatrix}\right) & W_{L_0} = \triangle\left(\begin{pmatrix}0\\ 0\end{pmatrix}, \begin{pmatrix}\sqrt{\tau}^3\\ -1\end{pmatrix}, \begin{pmatrix}\sqrt{\tau}\\ -\tau^2\end{pmatrix}\right) \\
W_{S_1} = \triangle\left(\begin{pmatrix}-\sqrt{\tau}\\ -\tau^2\end{pmatrix}, \begin{pmatrix}-\sqrt{\tau}^3\\ -1\end{pmatrix}, \begin{pmatrix}-\sqrt{\tau}^5\\ -\tau\end{pmatrix}\right) & W_{L_1} = \triangle\left(\begin{pmatrix}0\\ 0\end{pmatrix}, \begin{pmatrix}-\sqrt{\tau}^3\\ -1\end{pmatrix}, \begin{pmatrix}-\sqrt{\tau}\\ -\tau^2\end{pmatrix}\right) \\
W_{S_2} = \triangle\left(\begin{pmatrix}\sqrt{\tau}\\ \tau^2\end{pmatrix}, \begin{pmatrix}\sqrt{\tau}^3\\ 1\end{pmatrix}, \begin{pmatrix}\sqrt{\tau}^5\\ \tau\end{pmatrix}\right) & W_{L_2} = \triangle\left(\begin{pmatrix}0\\ 0\end{pmatrix}, \begin{pmatrix}\sqrt{\tau}^3\\ 1\end{pmatrix}, \begin{pmatrix}\sqrt{\tau}\\ \tau^2\end{pmatrix}\right) \\
W_{S_3} = \triangle\left(\begin{pmatrix}\sqrt{\tau}\\ -\tau^2\end{pmatrix}, \begin{pmatrix}\sqrt{\tau}^3\\ -1\end{pmatrix}, \begin{pmatrix}\sqrt{\tau}^5\\ -\tau\end{pmatrix}\right) & W_{L_3} = \triangle\left(\begin{pmatrix}0\\ 0\end{pmatrix}, \begin{pmatrix}-\sqrt{\tau}^3\\ 1\end{pmatrix}, \begin{pmatrix}-\sqrt{\tau}\\ \tau^2\end{pmatrix}\right)
\end{array}
\tag{51}
$$

is invariant under the internal inflation $\mathrm{infl}^*_{\boldsymbol{\mathcal{S}}_{\mathsf{A2}}}$.

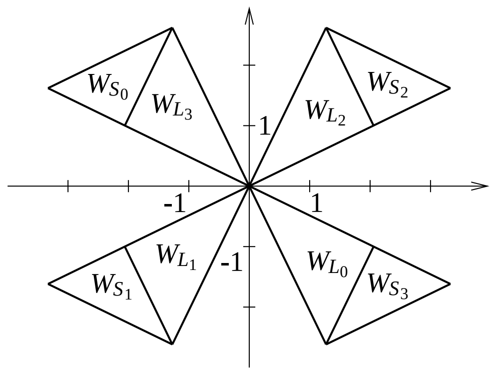

Figure 19: Windows for AMMANN tiling $\boldsymbol{\mathcal{S}}_{\mathsf{A2}}$

The size of the windows is again verified by the calculation of the density and formula (34). The density of the set of all control points of one tiling, is given by

$$
\mathrm{dens}(P) = \frac{1}{\tau^{-2}\,\mathrm{Vol}(S) + \tau^{-1}\,\mathrm{Vol}(L)} = \frac{2}{5}\sqrt{\tau}^3 \tag{52}
$$

because $\begin{pmatrix}\tau^{-2}\\ \tau^{-1}\end{pmatrix}$ gives as a right eigenvector of the inflation matrix $\left(\begin{smallmatrix}0&1\\1&1\end{smallmatrix}\right)$ the relative frequencies of the tiles S and L (and in each tile there is exactly one control point). This matches $\mathrm{Vol}(\bigcup W_{T,i})/\det(\Lambda) = \frac{2}{5}\sqrt{\tau}^3$, completing this outline for a proof of this projection setting for $\boldsymbol{\mathcal{S}}_{\mathsf{A2}}$ tilings.

Notice that the density of control points of any $\boldsymbol{\mathcal{S}}_{\mathsf{A2}}$ tiling is the same as the density of the vertex sets of the tilings in $\boldsymbol{\mathcal{S}}(\mathfrak{F}, \mathrm{infl})$ (with the above sizes of the prototiles) (cf. (34).

All edges of the window W for the vertex sets of $\boldsymbol{\mathcal{S}}(\mathfrak{F}, \mathrm{infl})$ tilings are horizontal or vertical, whereas edges of the windows $W_{T,i}$ for the control points of $\boldsymbol{\mathcal{S}}_{\mathsf{A2}}$ tilings are neither horizontal nor vertical. By the allowed reassembling operations (translations, $A \cup B$, $\overline{(A \cap B)^{\circ}}$ and $\overline{A \setminus B}$) no edges in new orientations can arise. Hence $\boldsymbol{\mathcal{S}}(\mathfrak{F}, \mathrm{infl})$ and $\boldsymbol{\mathcal{S}}_{\mathsf{A2}}$ are in different MLD-classes.

But there is another connection between the species $\boldsymbol{\mathcal{S}}_{\mathsf{A2}}$ and $\boldsymbol{\mathcal{S}}(\mathfrak{F}, \mathrm{infl})$: The inflation $\mathrm{infl}_{\mathsf{A2}}$ of $\boldsymbol{\mathcal{S}}_{\mathsf{A2}}$ is the Galois dual of the $\sqrt{-\tau}$ -inflation infl , see [8] Anhang B.5.

6.5 Fourier transform

For a fixed projection set define $\Delta = V(c) - V(c)$ and for $x \in \Delta$ let $\nu(x)$ be the density of points $y \in V(c)$ such that also $x + y \in V(c)$. Then the so-called autocorrelation distribution of $V(c)$ reads

$$\gamma_{V(c)} := \sum_{x \in \Delta} \nu(x) \delta_x \tag{53}$$

where δ_x is the Dirac-delta distribution settled at $x \in \mathbb{E}^2_P$. The amplitudes of the Fourier transform of this autocorrelation distribution are proportional to the intensity of the Bragg-Peaks observed in a diffraction experiment.

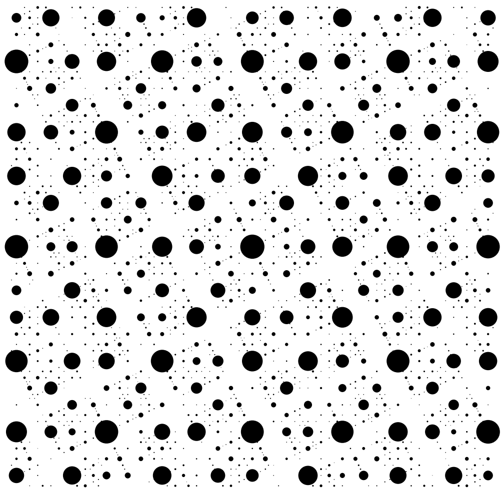

Figure 20: Calculation of the diffraction image of the vertex set of one tiling

As all projection sets $V(c)$ are in the same local isomorphism class, the Fourier transforms of their autocorrelation distributions are identically and given by

$$\hat{\gamma}_{\Lambda,W} = \sum_{z' \in \pi_P(\Lambda')} |A(z')|^2 \delta_{z'} \tag{54}$$

where $\Lambda' \in \mathbb{E}^4_S$ is the dual of the lattice Λ and the amplitudes $A(z')$ are

$$\begin{aligned} A(z') &= \frac{1}{\det(\Lambda)} \int_{-W} e^{-2\pi i \langle \pi^*(z'), y \rangle} dy \\ &= \frac{1}{10\tau} \cdot \frac{1}{\pi^2} \cdot \frac{\sin(2\pi\sqrt{\tau}^3 z'^*_1)}{z'^*_1} \cdot \frac{\sin(2\pi\tau z'^*_2)}{z'^*_2} \end{aligned} \tag{55}$$

where the z'^*_i are the two coefficients of $\pi^*(z')$ (cf. [14], [11] and references in the latter). Figure 20 shows this Fourier transform. The radii of the printed circles are proportional to the absolute values of the amplitudes, that is to say the area is proportional to the intensity of the Bragg peaks in a diffraction image. Only those spots are drawn, whose intensity is greater that 0.1% of the central one. Notice the both reflection symmetries, which are of course φ_1 and φ_2 defined in Section 2 and the almost self-similarity with expansion map β.

7 Concluding remarks, open questions

1. We think, it would be worth-while to search for species with similar properties for other *complex* PV - numbers instead of $\sqrt{-\tau}$ (e.g. $\eta = \sqrt{-(1+2\cos(\frac{2\pi}{7}))} \approx 1.498993\, \boldsymbol{i}$).

2. The atlas of the local matching rule lmr_c of Section 5.1 cannot be reduced to the atlas of couples of tiles, which share an edge or part of an edge. Therefore it is also impossible, to replace lmr_c by small alterations of the shapes (in five – resp. ten – different ways).

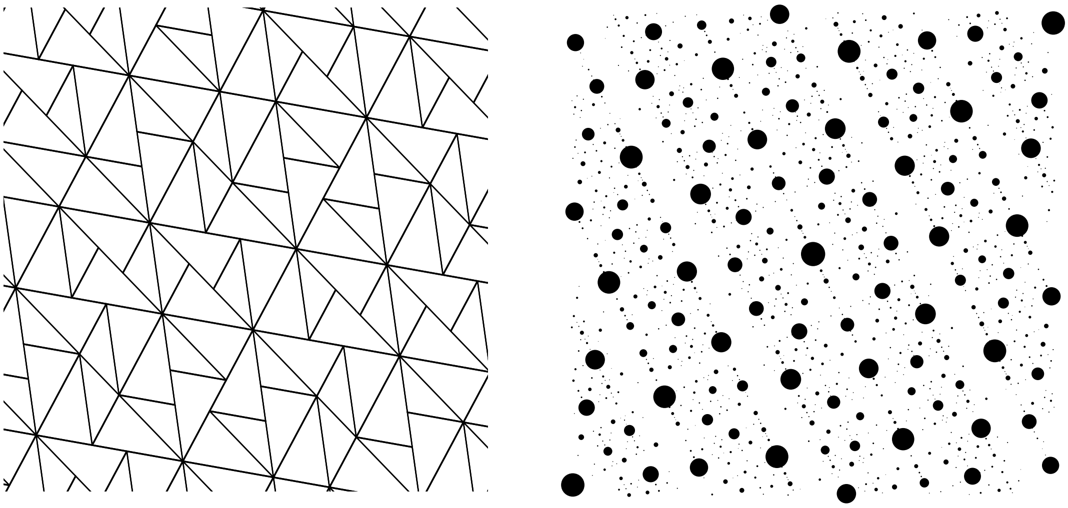

(a) Tiling (b) Fourier transform

Figure 21: Scaled $\sqrt{-\tau}$-tilings

3. If a tiling in $\boldsymbol{\mathcal{S}}(\mathfrak{F}, \mathrm{infl})$ is scaled by $1/\sqrt[4]{5}$ in the direction of the line of reflection of φ_1 (see Section 2), but not scaled in the perp direction (that of the line of reflection of φ_2), then the two tiles deform into two new tiles, the two Robinson triangles, which are the two isosceles triangles whose angles are multiples of $36°$; that is to say the two isosceles triangles, the edge lengths of which are 1 and τ (see Figure 21(a)). The Fourier transform shows an almost tenfold symmetry and it is near by hand to compare it with the Fourier transform of one of the decagonal species with the Robinson triangles. This is done in Figure 22 for the species $\boldsymbol{\mathcal{S}}_{\mathsf{TTT}}$ of so-called Tübingen Triangle Tilings (c.f. [4]).

The standard projection for $\boldsymbol{\mathcal{S}}_{\mathsf{TTT}}$ from a root lattice A_4 embedded in a five-dimensional space can easily be transfered to our projection setting, where we scale the physical space in φ_1-direction and also the internal space in the affiliated (horizontal) direction by $1/\sqrt[4]{5}$. Both the resulting windows are shown in Figure 23.

4. In addition to $\boldsymbol{\mathcal{S}}_{\mathsf{TTT}}$ there are other well-known examples of species with these two Robinson triangles, namely the Penrose-tilings in Robinsons triangulation

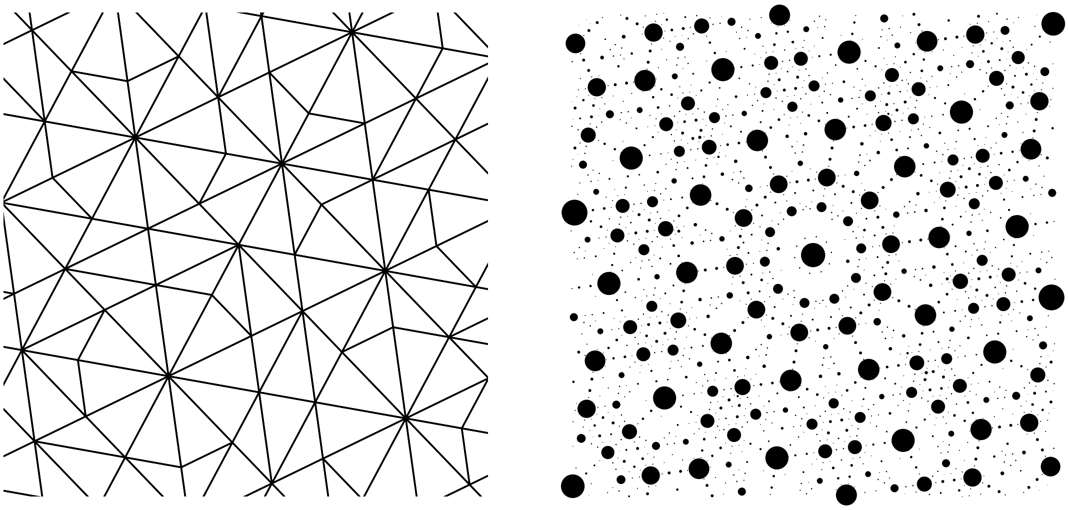

(a) Tiling (b) Fourier transform

Figure 22: “Tübingen Triangle Tiling”

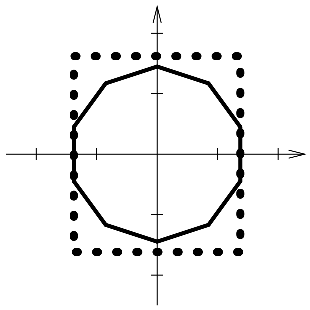

Figure 23: Windows (• • • scaled $\sqrt{-\tau}$ species, —— TTT)

($\boldsymbol{\mathcal{S}}_{\text{P-R}}$ cf. [1]) and the chiral tilings ($\boldsymbol{\mathcal{S}}_{\text{chiral}}$ cf. [3]). Table 2 shows the different inflation rules to the inflation factor τ . Notice that for the scaled $\sqrt{-\tau}$ species $\boldsymbol{\mathcal{S}}_{\text{scaled}}$ inflation with a linear factor $\sqrt{\tau}$ is no longer possible, because the tiles change their shape when β is applied. But the squared inflation is again a pure tile inflation. Here we may ignore the 180°-rotation of β^2 , because this rotation occurs already as orientation of the single tiles in the tiling.

5. In general there are essentially two types of inflation rules for the Robinson triangles with factor $\eta = \tau$ (cf. Table 3). The orientation of the isosceles prototiles A and B can be described by arrows along their bases. W.l.o.g. they can be chosen as shown in Table 3.

But in the supertiles one has $2^3 \times 2^2 = 32$ possibilities for either type. Precisely in 8 cases of either type the pseudo-supertile, which is contained in $\text{infl}(A)$ coincides with $\text{infl}(B)$, as it is the case for all four species mentioned in Table 2.

Species	Inflation of A 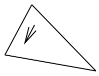	B 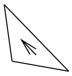	Remarks
$\boldsymbol{\mathcal{S}}_{\mathsf{scaled}}$	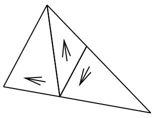	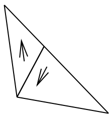	The tiles occur in only four different orientations, not 20 as in the other cases.
$\boldsymbol{\mathcal{S}}_{\mathsf{TTT}}$	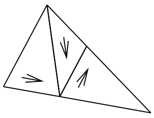	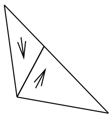	The tilings are vertex-to-vertex. No tiling with global D_5 symmetry.
$\boldsymbol{\mathcal{S}}_{\mathsf{chiral}}$	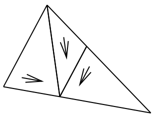	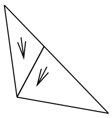	No reflection in the inflation, therefore at most ten different orientations of each tile.
$\boldsymbol{\mathcal{S}}_{\mathsf{P\text{-}R}}$	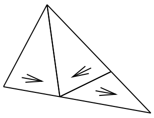	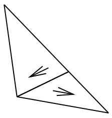	The tilings are vertex-to-vertex. There are two tilings with global D_5 symmetry.

Table 2: Well-known inflations for Robinson triangles

	A 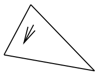	B 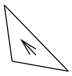
Type 1	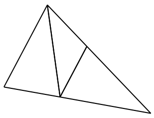	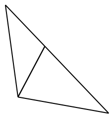
Type 2	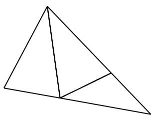	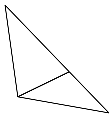

Table 3: Inflation rules for the Robinson triangles

Are there among these 64 cases some for which the resulting species are MLD to each other. How many different MLD classes are defined this way?

In which (how many) of the 64 cases is the resulting species vertex-to-vertex?

In which (how many) of those is it possible, to colour the vertices black and white in such a way, that white meets white and black meets black, as it is possible for $\boldsymbol{\mathcal{S}}_{\mathsf{P\text{-}R}}$?

Are there among these 64 species some w i t h o u t a unique deflation?

Are there others than the four species mentioned in Table 2, which deserve special interest?

6. The properties (A), (B), (C), (D) of the Appendix are possibly sufficient but probably not necessary for Theorem 2 to hold.

7. Under the assumption of (56), (57), (58), (61), and (69) we conjecture: If (C) is violated, then there are rectangles $\mathcal{R}_c(\underline{r}, \underline{r})$ in $\boldsymbol{\mathcal{S}}$ and hence (D) is also not true.

8. We conjecture, that five is the minimal number of colours in order to get a local matching rule for our original species.

Acknowledgement: We have to thank Dirk Frettlöh for a very careful reading of the manuscript and quite a few valuable comments.

8 Appendix

In this Appendix the algebraic background for the coloured inflation rule of Section 5.1 is presented. We do not want to give full proofs here, but restrict ourselves to a sketch of the ideas and the more important formulae.

We assume, we have k colours and describe the protoset by $\mathfrak{F}_c := \{1, 2, \ldots, k; \underline{1}, \underline{2}, \ldots, \underline{k}\}$, where the first k prototiles are congruent to A and the others congruent to X. Therefore all the following calculations are $\bmod k$.

For simplicity

$$\text{we assume } k \text{ to be an odd prime.} \tag{56}$$

Also for simplicity we consider only inflation rules given by linear maps. W.l.o.g. such a rule can be written as

$$\mathrm{infl}_c(n) := \underline{n}, \qquad \mathrm{infl}_c(\underline{n}) := (bn + y, \underline{an + x}) \qquad (1 \le n \le k). \tag{57}$$

We are looking for inflation rules with the following properties, which simplified the proof of Theorem 2 (essentially of the Lemma) considerably.

$$\mathfrak{F}_c \text{ shall be } \textit{minimal} \text{ with respect to } \mathrm{infl}_c \;^{14)}. \tag{A}$$

A necessary (but not sufficient) condition for (A) is

$$\gcd(b, k) = 1\,;\text{ under (56) this means: } b \not\equiv 0 \pmod{k} \;\; (a \text{ may vanish}). \tag{58}$$

The species $\boldsymbol{\mathcal{S}} := \boldsymbol{\mathcal{S}}(\mathfrak{F}_c, \mathrm{infl}_c)$ shall be invariant under a permutation group $\mathcal{A}ut_c$, which is transitive on the colours. (B)

All rectangles $\mathcal{R}_c(\underline{r}, \underline{s})$ occuring in $\boldsymbol{\mathcal{S}}$ shall be equivalent under $\mathcal{A}ut_c$. In other words: $s - r$ shall take – up to signature – only one value. (C)

In every rectangle $\mathcal{R}^3_c(\underline{r}, \underline{s})$ of $\boldsymbol{\mathcal{S}}$ there is at least one *pseudo*-supertile of second order. (D)

---

14) I.e.: There is no exponent q and no proper subset $\mathfrak{F}'_c$ of $\mathfrak{F}_c$, such that $\mathrm{infl}^q_c(\mathfrak{F}'_c) = \mathfrak{F}'_c$.

In order to find necessary (and partly sufficient) conditions on the coefficients a, b, x, y we first deduce some formulae from (57).

$$\mathrm{infl}_c^2(\underline{n}) = (\underline{bn+y}, abn+bx+y, \underline{a^2n+(a+1)x}), \tag{59}$$

$$\begin{aligned}\mathrm{infl}_c^3(\underline{n}) = \; &(b^2n+(b+1)y, \underline{abn+ay+x}, \underline{abn+bx+y}, \\ &a^2bn+(a+1)bx+y, \underline{a^3n+(a^2+a+1)x}).\end{aligned} \tag{60}$$

(59) shows, that (B) will hold if and only if

$$b \equiv a^2 \not\equiv 0 \pmod k \qquad \text{(cf. (58))}, \tag{61}$$

and then $\mathcal{A}ut_c$ is generated by $\pi := (1,2,\ldots,k)(\underline{m}, \underline{2m}, \ldots, \underline{km})$, where $m \equiv a^{-1} \pmod k$.

From now on we assume (56), (57) and (61) and get

$$\begin{aligned}\mathrm{infl}_c^3(\underline{n}) = \; &(a^4n+(a^2+1)y, \underline{a^3n+ay+x}, \underline{a^3n+a^2x+y}, \\ &a^4n+(a^3+a^2)x+y, \underline{a^3n+(a^2+a+1)x}),\end{aligned} \tag{60*}$$

$$\begin{aligned}\mathrm{infl}_c^4(\underline{n}) = \; &(a^4n+(a^2+1)y, \,.\,, \,.\,, \,.\,, \,.\,, \underline{a^4n+(a^3+a^2)x+y}, \,.\,, \\ &\underline{a^4n+(a^3+a^2+a+1)x}),\end{aligned} \tag{62}$$

and

$$\mathrm{infl}_c^6(\underline{n}) = (\ldots, \underbrace{\underline{a^6n+(a^5+a^4)x+(a^2+1)y}}_{\text{position } 14}, \ldots). \tag{63}$$

The first rectangles $\mathcal{R}_c(\underline{r}, \underline{s})$ occur in $\mathrm{infl}_c^3(\underline{n})$ and can be read off from (60*). This gives

$$r \equiv a^3n+ay+x, \quad s \equiv a^3n+a^2x+y \pmod k \text{ and} \tag{64}$$

$$\delta := s-r \equiv (a-1)((a+1)x-y) \pmod k \text{ independent on } n. \tag{65}$$

If $y \equiv (a+1)x$, then δ vanishes and in both corners of $\mathcal{R}_c^3(\underline{0}, \underline{0})$ we find the supertile $\mathrm{infl}^2(x)$, whence (D) is violated. Therefore

$$\left.\begin{array}{l}\text{we assume } y \equiv (a+1)x - c, \quad c \not\equiv 0 \pmod k \text{ and consequently} \\ \delta \equiv (a-1)c \pmod k.\end{array}\right\} \tag{66}$$

Assume $\mathcal{R}_c(\underline{t}, \underline{t+\varepsilon})$ occurs in $\boldsymbol{\mathcal{S}}$. Then we consider next the rectangles in the corners of $\mathcal{R}_c^4(\underline{t}, \underline{t+\varepsilon})$. Due to (B) it suffices to study the case $t \equiv 0$ and we find (cf. (62) and (66))

$$\mathcal{R}_c(\underline{(a^2+1)((a+1)x-c)}, \underline{a^4\varepsilon+(a^3+a^2+a+1)x})$$

and

$$\mathcal{R}_c(\underline{(a^3+a^2+a+1)x}, \underline{a^4\varepsilon+(a^2+1)((a+1)x-c}). \tag{67}$$

The differences turn out to be

$$a^4\varepsilon + (a^2+1)c \qquad \text{and} \qquad a^4\varepsilon - (a^2+1)c. \tag{68}$$

Since we want to realize (C), we require the two differences to be – up to signature – the same and we are lead to the following two cases.

Case 1: $(a^2+1)c \equiv 0 \pmod{k}$.

Then, applying (61), we arrive at

$$b \equiv a^2 \equiv -1 \pmod{k}. \tag{69}$$

This implies that both rectangles in the corners of $\mathcal{R}_c^4(\underline{0},\underline{\varepsilon})$ are equivalent to $\mathcal{R}_c(\underline{0},\underline{\varepsilon})$; and if (C) is valid, ε has to equal $\pm(a-1)((a+1)x-y)$.

Finally (cf. Fig. 9 and (63)) there occur new rectangles $\mathcal{R}_c(\underline{r},\underline{s})$ only in the center of $\mathcal{R}_c^6(\underline{t},\underline{t+\varepsilon})$. Due to (B) we may assume $t\equiv 0$ and find (cf. (69))

$$\begin{aligned}\mathcal{R}_c(\underline{(a^5+a^4)x+(a^2+1)y},\underline{a^6\varepsilon+(a^5+a^4)x+(a^2+1)y}) =\\ = \mathcal{R}_c(\underline{(a^5\dots)+\dots},\underline{-\varepsilon+((a^5\dots)+\dots)}),\end{aligned} \tag{70}$$

so there is no new difference.

Case 2: $a^4\varepsilon \equiv 0$ and $a^2 \not\equiv -1 \pmod{k}$.

Consequently $\varepsilon \equiv 0 \pmod{k}$ (cf. (61)). Then the new difference is $(a^2+1)c$ and with $\varepsilon \equiv (a^2+1)c$ we get the difference $2(a^2+1)c$ and so on. But if every residue class mod k is attained, then among the rectangles $\mathcal{R}_c^3(\underline{r},\underline{s})$ there is an equivalence class mod $\mathcal{A}ut_c$ violating (D).

The considerations of page 12 (cf. again Fig. 9) show: Under the assumption of (56), (57), (58) not only (61) is equivalent to (B), but (61), (66) and (69) also imply (C). It is not hard to prove, that these six assumptions also imply (A) and (D). Finally from (69) we can conclude

$$k \equiv -1 \pmod{4} \qquad \text{(in case } k=5 \text{ this implies } a\equiv \pm 2\text{)}. \tag{71}$$

For Section 5 we have chosen $k=5$ and $a\equiv 2$, $b\equiv -1$, $x\equiv y\equiv 1 \pmod{5}$.

References

[1] Raphael M. Robinson. Comments on the Penrose tiles. Mimeographed notes, September 1975. 8 pages.

[2] Branko Grünbaum and Geoffrey C. Shephard. *Tilings and Patterns.* Freeman, New York, 1987.

[3] C. Godrèche and J. M. Luck. Quasiperiodicity and randomness in tilings of the plane. *Journal of Statistical Physics*, **55**(1/2):1 – 28, 1989.

[4] Michael Baake, Peter Kramer, Martin Schlottmann, and D. Zeidler. Planar patterns with fivefold symmetry as sections of periodic structures in 4-space. *International Journal of Modern Physics B*, **4**(15&16):2217 – 2268, 1990.

[5] Michael Baake, Martin Schlottmann, and P. D. Jarvis. Quasiperiodic tilings with tenfold symmetry and equivalence with respect to local derivability. *Journal of Physics A (Mathematic and General)*, **24**:4637 – 4654, 1991.

[6] Charles Radin and M. Wolff. Space tilings and local isomorphism. *Geometriae Dedicata*, **42**:355 – 360, 1992.

[7] Charles Radin. The pinwheel tiling of the plane. *Annals of Math.*, **139**:661–702, 1994.

[8] Götz Gelbrich. *Gruppen, Parkette und Selbstähnlichkeit*. Verlag Dr. Kovač, Hamburg, 1995. Dissertation, Universität Greifswald.

[9] Michael Baake and Martin Schlottman. Geometric aspects of tilings and equivalent concepts. Preprint, 1996.

[10] Franz Gähler and R. Klitzing. The diffraction pattern of self-similar tilings. In Robert V. Moody, editor, *The Mathematics of Long-Range Aperiodic Order*, volume **489** of *NATO ASI Series C*, pages 141–174. Kluver, 1997.

[11] Albert Hof. Diffraction by aperiodic structures. In Robert V. Moody, editor, *The Mathematics of Long-Range Aperiodic Order*, volume **489** of *NATO ASI Series C*, pages 239–268. Kluver, 1997.

[12] Chaim Goodman-Strauss. Matching rules and substitution tilings. *Ann. Math.*, **147**(1):181–223, 1998.

[13] Martin Schlottmann. Cut-and-project sets in locally compact abelian groups. In Jiří Patera, editor, *Quasicrystals and Discrete Geometry*, volume **10** of *Fields Institute Monographs*, pages 247–264. AMS, 1998.

[14] Michael Baake. A guide to mathematical quasicrystals. Preprint, available in WWW at xxx.lanl.gov location math-ph/9901014, 1999.

Address of the authors: Fachbereich Mathematik
Universität Dortmund
D – 44221 Dortmund